DYNAMIC CONTACT OF TWO GAO BEAMS

JEONGHO AHN, KENNETH L. KUTTLER, MEIR SHILLOR

Abstract. The dynamic contact of two nonlinear Gao beams that are connected with a joint is modeled, analyzed, and numerically simulated. Contact is modeled with either (i) the normal compliance condition, or (ii) the unilateral Signorini condition. The model is in the form of a variational equality in case (i) and a variational inequality in case (ii). The existence of the unique variational solution is established for the problem with normal compliance and the existence of a weak solution is proved in case (ii). The solution in the second case is obtained as a limit of the solutions of the first case when the normal compliance stiffness tends to infinity. A numerical algorithm for the problem is constructed using finite elements and a mixed time discretization. Simulation results, based on the implementation of the algorithm, of the two cases when the horizontal traction vanishes or when it is sufficiently large to cause buckling, are presented. The spectrum of the vibrations, using the FFT, shows a rather noisy system.

1. Introduction

This work models the vibrations of two uniform elastic or viscoelastic nonlinear Gao beams that are connected with a mechanical joint that has a gap or clearance. The Gao nonlinear beam was introduced in [17, 18] to allow for the investigation of the vibrations of beams about buckled states. The model for the process is in the form of a system of nonlinear partial differential equations that are coupled across the joint. We establish the existence of a weak solution to the system. Then, we describe in detail a numerical algorithm for the problem, based on mixed finite elements, and present two typical numerical simulations. One deals with vibration when there is buckling, the other one without buckling. This is a step in our investigation of the noise properties of mechanical systems and the transmission of vibrations across joints.

Noise and vibration characteristics of mechanical assemblies, parts, and components are very important in industry. Currently, the automotive industry has considerable interest in the dynamic vibrations of mechanical systems, stemming from the customer's perception of noise characteristics of cars. The topic is under extensive research, mainly experimentally and in part computationally in the industry. However, there exists no complete methods for such investigation, and full

mathematical analysis of typical automotive problems is still out of reach. Therefore, most of the models use various ad hoc assumptions, many of which are too simplistic, and thus unrealistic, and not very useful.

Here, we introduce a simple one-dimensional geometrical setting to avoid certain mathematical complications related to two- or three-dimensions. On the other hand, the physical content of the problem is not simplified. Our long-term goal is to understand the transmission of vibrations across mechanical joints. This will help industry in the design of parts, assemblies and systems with acceptable noise and vibration characteristics. Eventually, theory will replace the current practice of finding that the system needs to be modified at the testing or even production stages, because of unacceptable noise generation.

Preliminary steps in this program have been taken in [9, 10, 25, 27] where various aspects of vibrations and contact of the Euler-Bernoulli linear beams were investigated. In particular the modeling, analysis, and simulations of the vibrations of a beam between two stops can be found in [9, 25, 27]. Here, we extend this study to include nonlinear beams, a fact that makes the analysis and computations much more complicated, since more specialized ideas and methods must be used.

Various mathematical and numerical results about the nonlinear Gao beam were reported in [4, 7, 8, 26, 33, 34, 31, 38]. The main interest there was to study the buckling of the beam and its vibrations about a buckled state. Contact conditions, even when the governing equations are linear, make the problems nonlinear, which led to the currently developing Mathematical Theory of Contact Mechanics ([21, 39] and references therein). Having a nonlinear equation and nonlinear contact conditions, again, makes the problem much harder, both in terms of its analysis and computationally. Computational issues related to contact can be found in [15, 21, 32, 37, 41]

Recent numerical schemes for dynamic contact problems of linear beams have been developed in [5, 2, 3]. In this paper, we propose a more advanced numerical algorithm that is more technical since we have to handle properly the nonlinear term in the equation. The theory of its convergence is investigated in [4]. Issues of control of the Gao beam can be found in [19, 20].

We assume, for the sake of generality, that the beams are viscoelastic, and describe the viscosity by a short-term memory of the Kelvin-Voigt type. Moreover, we also deal with the the inviscid case by passing to the limit when the viscosity vanishes. The dynamic contact is modeled by either the *Signorini nonpenetration condition* which describes *unilateral contact* of two perfectly rigid stops, or by the *normal compliance condition,* which describes reactive stops. This work is an extension of [8] where the problem of the vibrations of one Gao beam between two reactive stops was investigated. Some numerical simulations of the vibrations of two Euler-Bernoulli linear beams with a reactive joint problem can be found in [25], where the method of lines was used.

Next, we present a rather complex numerical algorithm for the problems. The complexity arises from the nonlinearity of the beam equation coupled with the nonlinear contact condition. The main idea of the numerical algorithm is to use time discretization and the combination of the central difference formula and the mixed finite element methods in space. Two simulations for the vibrations of the system when buckling takes place and when it is absent, are depicted, showing that the numerical scheme seem to be work reasonably well. The finite elements

naturally fit with the weak formulation of the problem, since this is their usual setting. We note that, adding to the complexity, it follows from the results of [35] that even a much simplified system of this type may exhibit chaotic behavior.

The rest of the work is organized as follows. In Section 2 we present the physical setting, and the classical model. We describe either the Signorini or the normal compliance contact conditions. The beams are assumed to be either viscoelastic or elastic. Since we allow the left beam to be fixed to an oscillating support, we introduce in Section 3 a change of variable that allows to consider a problem in which the left end is stationary. To present the variational formulation we introduce the relevant function spaces, and state our main existence results, the existence of the unique weak solution for the problem with normal compliance, Theorem 3.1, and an existence of a weak solution for the problem with the Signorini condition, Theorem 3.2.

In Section 4 we investigate the model with the normal compliance condition, which in addition to having its own merit, may be considered as regularization of the Signorini condition. We prove Theorem 3.1. In Section 5 we establish Theorem 3.2, in which a solution is obtained as a limit of a sequence of solutions found in Section 4. In Section 6 we show in Theorem 6.2 that the problems with the normal compliance condition or the Signorini condition with vanishing viscosity posses a weak solution, too. We obtain the necessary a priori estimates (Theorem 6.1) on the solutions with viscosity, and pass to the limit when the viscosity vanishes and the normal compliance stiffness coefficients tend to infinity.

We describe in Section 7 a numerical algorithm for the model, based on the mixed finite elements method. The central idea of the algorithm is to drive the recursive formula which enables to compute next time step solutions of the linear system per each step satisfying the contact conditions. The results of our simulations are given in Section 8. We present two sets of simulations without buckling ($p = 0$) and with the buckling of the right beam ($p = 895$). We also show the Fast Fourier Transform of the motion of the right end of the left beam, and the noise, i.e., the spectrum of frequencies that it generates.

The paper is summarized in Section 9, where some unresolved issues and future work are discussed, too.

2. The Model

This section presents the classical formulation of the model, a change of variable, the necessary function spaces, the variational form, and a statement of our theoretical results.

The physical setting, shown in Figure 2.1 and a detail of the joint in Figure 2.2, is as follows. Two uniform Gao beams are connected at at a joint with a clearance. The left beam is attached rigidly at its left end to a supporting device that may oscillate with time, possibly periodically. The right end of the second beam is clamped to a rigid support, say a wall. The motion of the right end of the left beam is constrained by the motion of the left end of beam 2, where it may move only within the given clearance. The expanded view of the joint is depicted in Figure 2.2, where g is the *clearance* or the *gap*. For the sake of generality we assume that the joint may be asymmetrical, and let $g = g_1 + g_2$ ($g_1, g_2 > 0$), where g_1 is the upper clearance and g_2 is the lower one, when the system is at rest.
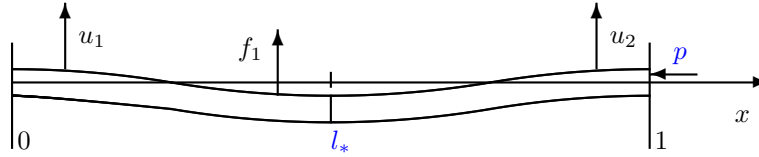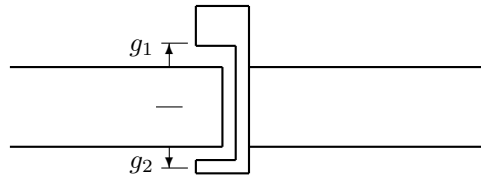
Figure 2.1: The two deflected Gao beams

Figure 2.2: The joint; $g = g_1 + g_2$ is the gap

The area-centers of gravity of the beams in their (stress free) dimensionless reference configurations coincide with the intervals $0 \le x \le l_*$, and $l_* \le x \le 1$, respectively.

A prescribed traction $p = p(t)$ acts at the right end $x = 1$; the beams' edges in the joint are assumed to be permanently in frictionless contact. Adding friction may be of interest in a future study.

We use dimensionless variables and denote by $u_1 = u_1(x,t)$ and $u_2 = u_2(x,t)$ the vertical displacements of the beams, and by $\sigma_i = \sigma_i(x,t)$ the shear stresses, for $i = 1, 2$, where here and below $i = 1$ indicates the left beam and $i = 2$ the right one. The equations of motion are

$$\rho_1 u_{1tt} - \sigma_{1x} = \rho_1 f_1, \quad 0 < x < l_*, \tag{2.1}$$

$$\rho_2 u_{2tt} - \sigma_{2x} = \rho_2 f_2, \quad l_* < x < 1, \tag{2.2}$$

where f_i denote the density (per unit mass) of the vertical applied forces, and ρ_i are the beams' densities (per unit length). Also, the subscripts x and t indicate partial derivatives. The time interval of interest is $0 \le t \le T$. The beams are nonlinear and the *constitutive relations* are,

$$\sigma_i(x,t) = -k_i u_{ixxx}(x,t) - d_i u_{itxxx}(x,t) + \frac{1}{3} a_i u_{ix}^3 - \overline{\nu_i} p u_{ix}, \tag{2.3}$$

where the k_i are the coefficients of elasticity, d_i are the coefficients of viscosity, a_i are the Gao coefficients, and $\overline{\nu_i}$ are positive coefficients related to the compressive or tensile traction, for $i = 1, 2$. By assumption, the beams are uniform and so the various coefficients are positive constants.

The initial conditions are

$$u_1(x,0) = u_{01}(x), \quad u_{1t}(x,0) = v_{01}(x) \quad 0 \le x \le l_*, \tag{2.4}$$

$$u_2(x,0) = u_{02}(x), \quad u_{2t}(x,0) = v_{02}(x) \quad l_* \le x \le 1, \tag{2.5}$$

where u_{0i} and v_{0i} are prescribed functions representing the initial deflections and velocities of the beams, respectively.

We suppose that the left beam is rigidly attached at its left end to a device that may be oscillating in time with vertical displacement ϕ, thus, for $0 \le t \le T$,

$$u_1(0, t) = \phi(t), \quad \text{and} \quad u_{1x}(0, t) = 0. \tag{2.6}$$

Here ϕ is known, and we have more to say about it below. The right end of the right beam is clamped, so

$$u_2(1, t) = 0, \quad \text{and} \quad u_{2x}(1, t) = 0. \tag{2.7}$$

We turn to describe the *contact process* in the joint. First, we model it with the *normal compliance* contact condition (see, e.g., [21, 22, 23, 24, 32, 39] and the references therein), which describes reactive stops. The contact shears satisfy

$$\sigma = \sigma(t) \equiv \sigma_1(l_*, t) = -\sigma_2(l_*, t). \tag{2.8}$$

When there is no contact the shear vanishes, thus,

$$u_2 - g_2 < u_1 < u_2 + g_1 \implies \sigma = 0.$$

The reaction of the stops takes place only when the displacement of the end of the left beam exceeds the clearance, is proportional to the interpenetration, and when

$$u_2(l_*, t) + g_1 \le u_1(l_*, t),$$

the reaction is

$$\sigma = -\lambda_1(u_1(l_*, t) - u_2(l_*, t), -g_1)$$

where $\lambda_1 > 0$ is the normal compliance stiffness of the top stop, and the reaction (acting on the edge of the left beam) is downward. When

$$u_1(l_*, t) \le u_2(l_*, t) - g_2,$$

the reaction is

$$\sigma = \lambda_2(u_2(l_*, t) - u_1(l_*, t) - g_2),$$

where $\lambda_2 > 0$ is the normal compliance stiffness of the lower stop, and the reaction (acting on the edge of the left beam) is upward. The discussion of the reaction of the stops can be summarized as follows,

$$\begin{aligned}
\sigma(t) &= \Lambda(u_1(l_*, t) - u_2(l_*, t)) \\
&\equiv -\lambda_1(u_1(l_*, t) - u_2(l_*, t) - g_1)_+ + \lambda_2(u_2(l_*, t) - u_1(l_*, t) - g_2)_+,
\end{aligned} \tag{2.9}$$

and $(f)_+ = \max(f, 0)$ is the positive part of the function.

We note that more general normal compliance power laws were introduced and used in [21, 6, 22, 23, 24, 32, 39], among many other references.

Finally, we assume that the ends do not exert moments on each other, and thus,

$$w_{ixx} = 0, \quad x = l_*. \tag{2.10}$$

Given the problem data; i.e., $u_{0i} = u_{0i}(x)$, $v_{0i} = v_{0i}(x)$, $(i = 1, 2)$, $p(t)$, and $\phi = \phi(t)$, the physical parameters and the constitutive relations (2.3), the *classical formulation of the dynamic contact at a joint of two Gao beams with the normal compliance contact condition* is:

Problem 2.1. *Find a pair of functions (u_1, u_2) such that (2.1)–(2.10) hold.*

The problem, in its variational form, is studied in Section 4 where we establish the existence of its unique weak solution.

The second contact condition that is often used is the so-called *Signorini non-penetration* or *unilateral* condition in which the stops are assumed to be *perfectly rigid*. It is, essentially, an idealization of the normal compliance condition, and may be justified in certain settings. We discuss the relationship between the conditions below.

Since the stops are rigid right, the right end of the left beam must be within the clearance of the left end of the right beam. Thus,

$$u_2(l_*, t) - g_2 \le u_1(l_*, t) \le u_2(l_*, t) + g_1.$$

When strict inequalities hold, there is no contact, the ends are free, and then $\sigma(t) = 0$. On the other hand, when the ends are in contact, the stresses are equal but opposite, then (2.8) holds.

Next, when contact takes place at the lower stop $u_1(l_*, t) = u_2(l_*, t) - g_2$ and $\sigma \ge 0$, and when the contact is at the upper stop, $u_1(l_*, t) = u_2(l_*, t) + g_1$ and $\sigma \le 0$. We may write it concisely by using the indicator function χ,

$$\chi(r) = \begin{cases} 0 & \text{if } u_2 - g_2 \le r \le u_2 + g_1, \\ +\infty & \text{otherwise.} \end{cases} \tag{2.11}$$

Then, we let $\partial\chi$ denote the *subdifferential* of χ, i.e.,

$$\partial\chi(r) = \begin{cases} 0 & \text{if } u_2 - g_2 < r < u_2 + g_1, \\ (-\infty, 0] & \text{if } r = u_2 - g_2, \\ [0, \infty) & \text{if } r = u_2 + g_1. \end{cases} \tag{2.12}$$

We note that the effective domain of both χ and $\partial\chi$ is $[u_2 - g_2, u_2 + g_1]$.

The contact conditions may be summarized in the form of the following set inclusion that represents the *complementary conditions*:

$$u_2 - g_2 \le u_1 \le \quad u_2 + g_1, \tag{2.13}$$
$$-\sigma \in \quad \partial\chi(u_1), \tag{2.14}$$

evaluated at $x = l_*$, together with (2.8).

Given the problem data, i.e., $u_{0i} = u_{0i}(x)$, $v_{0i} = v_{0i}(x)$, $(i = 1, 2)$, p, and $\phi = \phi(x)$, the physical parameters and the constitutive relations (2.3), the 'classical' formulation of *the dynamic contact of two Gao beams with the Signorini contact condition* is:

Problem 2.2. *Find a pair of functions (u_1, u_2) such that (2.1)–(2.8), (2.10) and (2.13)–(2.14) hold.*

However, the Signorini condition is an over-idealization when dynamic contact takes place [39]. In the literature, the normal compliance condition is often used as a regularization of the Signorini condition, although physically, the Signorini condition seems to be an idealization of the normal compliance condition, as there are no perfectly rigid objects. Moreover, the Signorini condition introduces sever mathematical difficulties in multidimensional dynamic contact problems, that reflect the fact that there are no perfectly rigid objects. Moreover, there are issues of energy conservation when using it [5, 37]. The Signorini condition can be obtained (formally) as a limit when the stiffness in the normal compliance condition tends

to infinity. This has been established rigorously in many works, see, e.g., [16, 28] and the references therein. Indeed, in this work and establish the solvability of the problem with the Signorini condition in the limit $\lambda_1, \lambda_2 \to \infty$. However, we do it mainly to show that the normal compliance problems behave well even when the stiffnesses are arbitrarily large and, also, for the sake of completeness.

3. Variational formulation and results

We proceed to a weak or variational formulation of the two problems, since the solutions may not be sufficiently regular. Indeed, this is the case in the problem with the Signorini condition since the velocity is discontinuous upon impact. Moreover, there is regularity ceiling for the problem with normal compliance (see [29] for the details). More importantly, we use it since the mathematical tools for weak solutions are much more advanced. Moreover, the variational formulation is the basis for the finite element algorithm presented in Section 7.

We turn to introduce the function spaces that are needed. However, first we change the variable u_1 so as to have a zero boundary condition at $x = 0$, so that the function spaces we use below that incorporate the boundary conditions do not depend on time. To that end, we introduce a smooth function $\Phi = \Phi(x,t)$, for $0 \le x \le l_*$, such that

$$\Phi(0,t) = \phi(t), \quad \Phi_x(0,t) = 0,$$
$$\Phi(l_*,t) = \Phi_x(l_*,t) = \Phi_{xx}(l_*,t) = \Phi_{xxx}(l_*,t) = 0. \tag{3.1}$$

We note that the function

$$\Phi(x,t) = \phi(t) \cos^4\left(\frac{\pi x}{2l_*}\right)$$

satisfies all these conditions. The new dependent variable

$$\overline{u}_1(x,t) = u_1(x,t) - \Phi(x,t), \tag{3.2}$$

satisfies,

$$\overline{u}_1(0,t) = \overline{u}_{1x}(0,t) = 0,$$
$$\overline{u}_1(l_*,t) = \overline{u}_{1x}(l_*,t) = \overline{u}_{1xx}(l_*,t) = \overline{u}_{1xxx}(l_*,t) = 0.$$

These properties guarantee that the contact conditions in terms of $\overline{u}_1$ remain the same as above.

We perform the same change of the initial condition u_{10} and v_{10}.

The shear stress in the first beam may be written as

$$\sigma_1(x,t) = -k_1\overline{u}_{1xxx} - d_1\overline{u}_{1txxx} + \frac{1}{3}a_1(\overline{u}_{1x} + \Phi_x)^3$$
$$- \overline{\nu}_1 p\overline{u}_{1x} + \Psi(x,t,p), \tag{3.3}$$

where we set

$$\Psi(x,t,p(t)) = -k_1\Phi_{xxx} - d_1\Phi_{txxx} - \overline{\nu}_1 p\Phi_x. \tag{3.4}$$

We note that $\Psi(l_*,t,p(t)) = 0$, so that the change of the variable does not change the contact shear stress.

Next, we rewrite the force as

$$\overline{f}_1 = f_1 - \ddot{\phi}(t) \cos^4\left(\frac{\pi x}{2l_*}\right).$$

For the sake of simplicity, we do not use the bar below, and so u_1 denotes $\bar{u}_1(x,t)$ and f_1 stands for $\bar{f}_1$, so that the equation of motion (2.1) remains the same. We also rescale the variables so that $\rho_1 = \rho_2 = 1$ for the sake of simplicity of the presentation.

We now proceed to the variational formulation of the problem. We use the following notation:

$$V_1 \equiv \{w \in H^2(0, l_*) : w(0) = w_x(0) = 0\},$$
$$V_2 \equiv \{w \in H^2(l_*, 1) : w(1) = w_x(1) = 0\}.$$

We note that the transformation of u_1 allows us to make V_1 independent of time. Also,

$$H_1 \equiv L^2(0, l_*), \quad H_2 \equiv L^2(l_*, 1).$$

Let $V \equiv V_1 \times V_2$ and $H \equiv H_1 \times H_2$. Then, identifying H and H', we may write,

$$V \subseteq H = H' \subseteq V'.$$

Let $\mathcal{V}_i \equiv L^2(0, T; V_i)$, $\mathcal{H}_i \equiv L^2(0, T; H_i)$, for $i = 1, 2$, and $\mathcal{V} \equiv L^2(0, T; V)$, and $\mathcal{H} \equiv L^2(0, T; H)$, for $T > 0$. We denote by $(v, v)_{H_i}$ the inner product on H_i and the norm by $|v|^2_{H_i} = (v, v)_{H_i}$, for $i = 1, 2$. The inner products and norms on the other spaces are defined similarly. On $\mathcal{V}$ we may use the equivalent norm

$$\|\mathbf{v}\| = |\mathbf{v}_{xx}|_H,$$

and we do so when it is convenient. We also define

$$W_1 \equiv \{w \in H^1(0, l_*) : w(0) = 0\}, \quad W_2 \equiv \{w \in H^1(l_*, 1) : w(1) = 0\},$$

with similar notation as above.

Let $\mathbf{w} = (w_1, w_2) \in \mathcal{V}$, and let $\phi \in C^\infty([0, T])$ with $\phi(T) = 0$. We multiply (2.1) with $w_1(x)\phi(t)$ and integrate (formally) over $(0, l_*) \times (0, T)$, and integrating by parts we obtain the following variational equations for u_1,

$$
\begin{aligned}
&- (v_{01}, w_1)_{H_1}\phi(0) - \int_0^T (u_{1t}, w_1)_{H_1}\phi'(t)dt \\
&- \int_0^T (\sigma_1(l_*)w_1(l_*) + (k_1 u_{1xx} + d_1 u_{1txx}, w_{1xx})_{H_1})\phi(t)dt \\
&+ \frac{1}{3}a_1 \int_0^T \left((u_{1x} + \Phi_x)^3, w_{1x}\right)_{H_1} \phi(t)\,dt \\
&+ \int_0^T (-\bar{\nu}_1 p(t)(u_{1x}, w_{1x})_{H_1} - (\Psi_x, w_1)_{H_1})\phi(t)\,dt \\
&= \int_0^T (f_1, w_1)_{H_1}\phi(t).
\end{aligned}
\tag{3.5}
$$

Similarly, we multiply (2.2) with $w_2(x)\phi(t)$, integrate over $(l_*, 1) \times (0, T)$ and find

$$
\begin{aligned}
& -(v_{02}, w_2)_{H_2}\phi(0) - \int_0^T (u_{2t}, w_2)_{H_1}\phi'(t)dt \\
& + \int_0^T (\sigma_2(l_*)w_2(l_*) + (k_2 u_{2xx} + d_2 u_{2txx}, w_{2xx})_{H_2})\phi(t)dt \\
& + \int_0^T ((\frac{1}{3}a_2 u_{2x}^3 - \bar{\nu}_2 p(t)u_{2x}), w_{2x})_{H_2}\phi(t)dt \\
& = \int_0^T (f_2, w_{2s})_{H_2}\phi(t)dt
\end{aligned}
\tag{3.6}
$$

Here, the shear stresses $\sigma_1(l_*)$ and $\sigma_2(l_*)$ satisfy (2.8) and either the normal compliance condition (2.9) or the Signorini condition (2.13) and (2.14).

The convex set of admissible pairs of displacements is

$$
\begin{aligned}
K = \big\{ \mathbf{w} = (w_1, w_2) \in V : w_1(0) = 0, w_2(1) = 0, \\
w_2(l_*) - g_2 \le w_1(l_*) \le w_2(l_*) + g_1 \big\}.
\end{aligned}
\tag{3.7}
$$

and we set $\mathcal{K} = L^2(0, T; K)$.

We make the following assumptions on the problem data:

(A1) The initial displacements $\mathbf{u}_0 = (u_{01}, u_{02})$ and velocities $\mathbf{v}_0 = (v_{01}, v_{02})$ satisfy

$$
\mathbf{u}_0 \in K, \quad \mathbf{v}_0 \in H.
\tag{3.8}
$$

(A2) The traction $p = p(t)$ satisfies

$$
p \in C^1([0, T]), \quad |p|, |p'| \le p_0.
\tag{3.9}
$$

(A3) The motion of the left support $\phi = \phi(t)$ satisfies

$$
\phi \in C^2([0, T]), \quad u_{01}(0) = \phi(0).
\tag{3.10}
$$

(A4) The body forces $\mathbf{f} = (f_1(x, t), f_2(x, t))$ satisfy

$$
\mathbf{f} \in H.
\tag{3.11}
$$

(A5) The coefficients

$$
g_1, g_2, k_i, d_i, a_i, \bar{\nu}_i, \lambda_i, \quad i = 1, 2,
\tag{3.12}
$$

are positive constants.

The main theoretical result in this work is the following existence and uniqueness result for the problem with the normal compliance contact condition.

Theorem 3.1. *Assume that* (A1)–(A5) *hold. Then, there exists a unique solution* $\mathbf{u} = (u_1, u_2) \in \mathcal{V}$, *such that* $\mathbf{u}(\cdot, 0) = \mathbf{u}_0$, $\mathbf{u}_t(\cdot, 0) = \mathbf{v}_0$, *and the variational equations* (3.5) *and* (3.6) *hold. The stress* $\sigma(t)$ *satisfies* (2.9) *in a weak sense.*

The proof of the theorem is presented in Section 4. We conclude that Problem 2.1 has a unique weak solution.

In the case of the Signorini condition, we consider the following variational formulation of the problem to find $\mathbf{u}, \mathbf{v} \in \mathcal{V}$ such that if $\mathbf{w}, \mathbf{w}' \in \mathcal{V}$ is such that $\mathbf{w}(T) = \mathbf{u}(T)$ and

$$
-g_2 \le w_1(l_*, t) - w_2(l_*, t) \le g_1,
$$

then,

$$(\mathbf{v}_0, \mathbf{w}(0) - \mathbf{u}_0)_H - \int_0^T (\mathbf{v}, \mathbf{v} - \mathbf{w}')_H dt$$

$$+ \int_0^T \left(\left(\int_0^{l_*} k_1 u_{1xx}(u_{1xx} - w_{1xx}) dx \right) + \left(\int_{l_*}^1 k_2 u_{2xx}(u_{2xx} - w_{2xx}) dx \right) \right) ds$$

$$+ \int_0^T \left(\left(\int_0^{l_*} d_1 v_{1xx}(u_{1xx} - w_{1xx}) dx \right) + \left(\int_{l_*}^1 d_2 v_{2xx}(u_{2xx} - w_{2xx}) dx \right) \right) ds$$

$$+ \int_0^T \frac{1}{3} a_1 \left((u_{1x} + \Phi_x)^3, u_{1x} - w_{1x} \right)_{H_1} - \overline{\nu}_1 (p u_{1x}, u_{1x} - w_{1x})_{H_1} dt$$

$$+ \int_0^T -(\Psi_x, u_1 - w_1)_{H_1} \frac{1}{3} a_2 \left(((u_{2x})^3 - \nu_2 p u_{2x}), u_{2x} - w_{2x} \right)_{H_2} dt$$

$$\leq \int_0^T (\mathbf{f}, \mathbf{u} - \mathbf{w})_H ds.$$

The existence result for the problem with the Signorini condition is:

Theorem 3.2. *Assume that* (A1)–(A5) *hold. Then, there exists a function* $\mathbf{u} = (u_1, u_2) \in \mathcal{K}$, *such that* $\mathbf{u}(\cdot, 0) = \mathbf{u}_0$, $\mathbf{u}_t(\cdot, 0) = \mathbf{v}_0$, *and for a.a.* $t \in (0, T)$ *the variational equations* (3.5) *and* (3.6) *hold, together with* (2.13) *and* (2.14).

The theorem is established in Section 5, and is based on obtaining the necessary a priori estimates on the solutions of the problems with normal compliance and passing to the limit as the normal compliance stiffnesses become rigid; i.e., $\lambda_1, \lambda_2 \to \infty$.

We conclude that Problem 2.2 has a weak solution and note that, quite typically, the uniqueness of the solution is an unresolved question.

We also note that the corresponding problems without viscosity have variational solutions, too, see Section 6, however their uniqueness is open.

4. The problem with normal compliance

We establish Theorem 3.1 by transforming the variational equation into an abstract evolution equation in $\mathcal{V}'$ to which we apply various results for such abstract equations. To deal with the cubic terms in the constitutive relations (2.3) we introduce a truncation. For detailed description of the various Sobolev Spaced used here, we refer to [1].

First, we depict in Figure 4.1 the normal compliance condition (2.9) with the Lipschitz continuous function Λ, and the contact shear is given by

$$\sigma(t) = \Lambda(u_1(l_*, t) - u_2(l_*, t)). \tag{4.1}$$

When we study the problem with the Signorini condition, in the following section, we let $\lambda_1, \lambda_2 \to \infty$ leading the multifunction $\Lambda_\infty = \partial \chi$ given in (2.12) and depicted in Figure 5.1.

To deal with the nonlinear cubic term, we use truncation and replace the function $Q(r) = r^3$ with

$$Q_m(r) \equiv \begin{cases} m^3 & \text{if } r > m \\ r^3 & \text{if } |r| \leq m \\ -m^3 & \text{if } r < -m \end{cases} \tag{4.2}$$
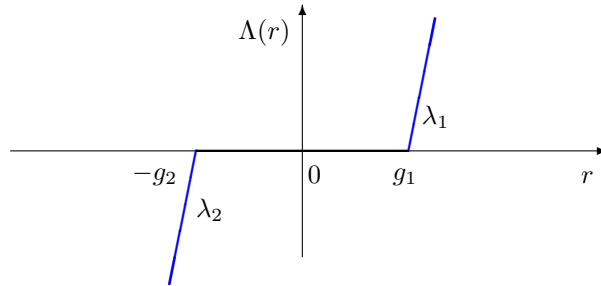
Figure 4.1: The normal compliance graph, the slopes are λ_i, $i = 1, 2$, $r = 0$ corresponds to the center at $u_2(l_*, t)$

Integration of (3.5) and (3.6) in time over $(0, T)$ leads to the approximate problem of finding, for a fixed $m > 0$, a pair $\mathbf{u}_m = (u_{1m}, u_{2m}) \in \mathcal{V}$ such that

$$
\begin{aligned}
&\langle u_{1tt}, w_1 \rangle_{\mathcal{V}_1} - \int_0^T \sigma(t) w_1(l_*) \, dt + (k_1 u_{1xx} + d_1 u_{1txx}, w_{1xx})_{\mathcal{H}_1} \\
&+ \frac{1}{3} a_1 (Q_m(u_{1x} + \Phi_x), w_{1x})_{\mathcal{H}_1} - \overline{\nu}_1 (p u_{1x}, w_{1x})_{\mathcal{H}_1} - (\Psi_x, w_1)_{\mathcal{H}_1} \\
&= (f_1, w_1)_{\mathcal{H}_1},
\end{aligned}
\tag{4.3}
$$

and

$$
\begin{aligned}
&\langle u_{2tt}, w_2 \rangle_{\mathcal{V}_2} - \int_0^T \sigma(t) w_2(l_*) \, dt + (k_2 u_{2xx} + d_2 u_{2txx}, w_{2xx})_{\mathcal{H}_2} \\
&+ \frac{1}{3} a_2 ((Q_m(u_{2x}) - \overline{\nu}_2 p u_{2x}), w_{2x})_{\mathcal{H}_2} \\
&= (f_2, w_2)_{\mathcal{H}_2},
\end{aligned}
\tag{4.4}
$$

where we used condition (2.8) for σ, along with the initial conditions $\mathbf{u}(\cdot, 0) = \mathbf{u}_0$, $\mathbf{u}_t(\cdot, 0) = \mathbf{v}_0$. Here, $w_i \in \mathcal{V}_i$ and the time derivatives are understood in the sense of V_i' valued distributions.

Let $\mathbf{u} = (u_1, u_2) \in \mathcal{V}$, we use the notation

$$
\mathbf{v} = \mathbf{u}', \quad \mathbf{u}(t) = \mathbf{u}_0 + \int_0^t \mathbf{v}(s) \, ds,
$$

where here and below the prime denotes the partial t derivative. We use the notation γ for the trace map from V on $x = l_*$ and the projection $\pi_i \mathbf{u} \equiv u_i$, for $i = 1, 2$, and γ^* is the adjoint map of γ. Next, we define the operators $A, B, N_m(t, \cdot) : V \to V'$ by

$$
\langle A\mathbf{v}, \mathbf{w} \rangle \equiv \left(\int_0^{l_*} d_1 v_{1xx} w_{1xx} dx \right) + \left(\int_{l_*}^1 d_2 v_{2xx} w_{2xx} dx \right),
\tag{4.5}
$$

$$
\langle B\mathbf{u}, \mathbf{w} \rangle \equiv \left(\int_0^{l_*} k_1 u_{1xx} w_{1xx} dx \right) + \left(\int_{l_*}^1 k_2 u_{2xx} w_{2xx} dx \right),
\tag{4.6}
$$

and

$$\langle N_m(t, \mathbf{u}), \mathbf{w} \rangle = \frac{1}{3} a_1 (Q_m(u_{1x} + \Phi_x), w_{1x})_{H_1} - \overline{\nu}_1 (pu_{1x}, w_{1x})_{H_1}$$
$$- (\Psi_x, w_1)_{H_1} + \frac{1}{3} a_2 ((Q_m(u_{2x}) - \overline{\nu}_2 pu_{2x}), w_{2x})_{H_2}. \tag{4.7}$$

Here and below, $\langle \cdot, \cdot \rangle$ denotes the duality pairing between V and V' and we consider these operators as also being defined on $\mathcal{V}$ in the obvious way.

Then, (3.5) and (3.6), along with the initial conditions, can be written as an abstract equation in $\mathcal{V}'$ as follows:

Problem 4.1. Find a pair $\mathbf{u}_m, \mathbf{v}_m \in \mathcal{V}$ with $\mathbf{v}'_m \in \mathcal{V}'$, for integer $m > 0$, such that,

$$\mathbf{v}' + A\mathbf{v} + B\mathbf{u} + N_m(\cdot, \mathbf{u}) + \pi_1^* \gamma^* \Lambda(u_1(l_*, \cdot) - u_2(l_*, \cdot))$$
$$- \pi_2^* \gamma^* \Lambda(u_1(l_*, \cdot) - u_2(l_*, \cdot)) = \mathbf{f}, \tag{4.8}$$

$$\mathbf{v}(0) = \mathbf{v}_0, \tag{4.9}$$

$$\mathbf{u}(t) = \mathbf{u}_0 + \int_0^t \mathbf{v}(s) ds. \tag{4.10}$$

Here, and below, we omit the subscript m from the solution, until we need it in passing to the limit $m \to \infty$.

We note that the operator N_m is Lipschitz continuous, and satisfies

$$\|N_m(t, \mathbf{u}) - N_m(t, \mathbf{w})\|_{V'} \leq K_m \|\mathbf{u} - \mathbf{w}\|_V,$$

where the constant K_m which is independent of t.

Also, let $N(t, \mathbf{u}) : V \to V'$ be defined by

$$\langle N(\cdot, \mathbf{u}), \mathbf{w} \rangle = \frac{1}{3} a_1 ((u_{1x} + \Phi_x)^3, w_{1x})_{H_1} - \overline{\nu}_1 (pu_{1x}, w_{1x})_{H_1}$$
$$- (\Psi_x, w_1)_{H_1} + \frac{1}{3} a_2 (((u_{2x})^3 - \nu_2 pu_{2x}), w_{2x})_{H_2}. \tag{4.11}$$

Next, let

$$R_m(r) = \int_0^r Q_m(z) dz,$$

Moreover, using assumption (A2), we obtain

$$\int_0^t p(s)(u_{1x}, u_{1tx})_{H_1} ds = \frac{1}{2} \int_0^t p(s) \frac{d}{ds} |u_{1x}|_{H_1}^2$$

$$\geq -p_0 |u_{1x}(t)|_{H_1}^2 - C(p(0), u_{01}) - p_0 \int_0^t |u_{1x}(s)|_{H_1}^2 ds.$$

This implies that for suitable $\delta > 0$, depending only on a_1 and a_2, we can derive the estimate

$$\int_0^t \langle N_m(s, \mathbf{u}(s)), \mathbf{v}(s) \rangle ds$$

$$\geq \delta \int_0^{l_*} R_m(u_{1x}(t) + \Phi_x(t)) dx - \frac{a_1}{3} \int_0^t (Q_m(u_{1x} + \Phi_x), \Phi'_x)_{H_1} dt$$

$$+ \delta \int_{l_*}^1 R_m(u_{2x}(t)) dx - C(u_{10}, \Phi_x(0, \cdot), \Phi_x) - (2 + p_0) \int_0^t \int_0^{l_*} |u_{1x}|^2 dx \, ds$$

$$- C(\Psi_x, \Psi_{tx}, \Psi_x(0, \cdot)) - C(p)|u_{1x}(t)|_{H_1}^2.$$

Consider that second term on the right of the inequality.

$$\left| \int_0^t (Q_m(u_{1x} + \Phi_x), \Phi'_x)_H dt \right| \leq C(\Phi'_x) \int_0^t \int_0^{l_*} Q_m(|u_{1x} + \Phi_x|)\, dx\, ds + C(\Phi'_x, \Phi_x).$$

Then, adjusting the constants, we find

$$\leq C(\Phi'_x) \int_0^t \int_0^{l_*} R_m(u_{1x} + \Phi_x)\, dx\, ds + C(\Phi'_x, \Phi_x).$$

It follows that

$$\int_0^t \langle N_m(s, \mathbf{u}(s)), \mathbf{v}(s) \rangle ds$$

$$\geq \delta \int_0^{l_*} R_m(u_{1x}(t) + \Phi_x(t)) dx - C(\Phi'_x) \int_0^t \int_0^{l_*} R_m(u_{1x} + \Phi_x)\, dx\, ds$$

$$- C(\Phi'_x, \Phi_x) + \delta \int_{l_*}^1 R_m(u_{2x}(t)) dx - C(u_{10}, \Phi_x(0, \cdot), \Phi_x)$$

$$- (2 + p_0) \int_0^t \int_0^{l_*} |u_{1x}|^2\, dx\, ds - C(\Psi_x, \Psi_{tx}, \Psi_x(0, \cdot)) - C(p)|u_{1x}(t)|^2_{H_1}.$$

Written in a simpler form, we have,

$$\int_0^t \langle N_m(s, \mathbf{u}(s)), \mathbf{v}(s) \rangle ds$$

$$\geq \delta \int_0^{l_*} R_m(u_{1x}(t) + \Phi_x(t)) dx + \delta \int_{l_*}^1 R_m(u_{2x}(t)) dx$$

$$- C(p) \int_0^t \|\mathbf{u}\|^2_W ds - C(p)\|\mathbf{u}(t)\|^2_W - C \int_0^t \int_0^{l_*} R_m(u_{1x} + \Phi_x)\, dx\, ds - C,$$

$$(4.12)$$

where the constants depend on the initial data and the given functions, but not on a_i, d_i or k_i, $i = 1, 2$.

The following existence and uniqueness result holds for each integer m.

Lemma 4.2. *For each positive integer m, there exists a unique solution $(\mathbf{u}_m, \mathbf{v}_m)$ to Problem 4.1.*

Proof. For the sake of convenience, let the operator $M(\cdot, \mathbf{u})$ be defined as

$$B\mathbf{u} + N_m(\cdot, \mathbf{u}) + \pi_1^* \gamma^* \Lambda(u_1(l_*) - u_2(l_*)) - \pi_2^* \gamma^* \Lambda(u_1(l_*) - u_2(l_*)),$$

so that M is Lipschitz as a map from $\mathcal{V}$ to $\mathcal{V}'$ with a constant K depending on m and λ_1, λ_2.

For $\mathbf{u_1} \in \mathcal{V}$, let $\mathbf{v}_1$ be the solution of

$$\mathbf{v}'_1 + A\mathbf{v}_1 + M(t, \mathbf{u}_1) = \mathbf{f}, \quad \mathbf{v}_1(0) = \mathbf{v}_0.$$

Then, let $\mathbf{w}_1$ be given by

$$\mathbf{w}_1(t) = \mathbf{u}_0 + \int_0^t \mathbf{v}_1(s) ds.$$

Consider the map $\mathbf{u}_1 \to \mathbf{v}_1 \to \mathbf{w}_1$. Consider $\mathbf{u}_1, \mathbf{u}_2$ and the corresponding $\mathbf{w}_i$ that result in this way. First, from the equation, we have

$$\frac{1}{2}|\mathbf{v}_1(t) - \mathbf{v}_2(t)|_H^2 + \delta \int_0^t \|\mathbf{v}_1(s) - \mathbf{v}_2(s)\|_V^2 ds$$

$$\leq \int_0^t \langle M(s, \mathbf{u}_1) - M(s, \mathbf{u}_1), \mathbf{v}_1(s) - \mathbf{v}_2(s) \rangle ds$$

$$\leq C \int_0^t \|\mathbf{u}_1(s) - \mathbf{u}_2(s)\|_V^2 ds + \frac{\delta}{2} \int_0^t \|\mathbf{v}_1(s) - \mathbf{v}_2(s)\|_V^2 ds,$$

and so

$$|\mathbf{v}_1(t) - \mathbf{v}_2(t)|_H^2 + \int_0^t \|\mathbf{v}_1(s) - \mathbf{v}_2(s)\|_V^2 ds \leq C \int_0^t \|\mathbf{u}_1(s) - \mathbf{u}_2(s)\|_V^2 ds.$$

Now, it follows from the definition of $\mathbf{w}_i$ and the above inequality, that

$$\|\mathbf{w}_1(t) - \mathbf{w}_2(t)\|_V^2 \leq C(T) \int_0^t \|\mathbf{v}_1(s) - \mathbf{v}_2(s)\|_V^2 ds$$

$$\leq C \int_0^t \|\mathbf{u}_1(s) - \mathbf{u}_2(s)\|_V^2 ds.$$

Iterating this inequality sufficient number of times shows that a high enough power of this map is a contraction map on $\mathcal{V}$. Therefore, it has a unique fixed point $\mathbf{u}$ which yields the unique solution to Problem 4.1. $\square$

Next, we derive the necessary estimates that are independent of m. We denote by $(\mathbf{u}_m, \mathbf{v}_m)$ the solution guaranteed in Lemma 4.2, however, below we omit the subscript m.

From (4.8) and the estimate given for N_m in (4.12), it follows that there exists a constant $\delta > 0$, depending on the parameters of the problem, such that

$$\frac{1}{2}|\mathbf{v}(t)|_H^2 + \min(d_1, d_2) \int_0^t \|\mathbf{v}(s)\|_V^2 ds + \min(k_1, k_2)\|\mathbf{u}(t)\|_V^2$$

$$+ \delta \int_0^{l_*} R_m(u_{1x}(t) + \Phi_x(t))dx + \delta \int_{l_*}^1 R_m(u_{2x}(t))dx$$

$$+ \int_0^t \Lambda(u_1(s, l_*) - u_2(s, l_*))(v_1(s, l_*))ds$$

$$- \int_0^t \Lambda(u_1(s, l_*) - u_2(s, l_*))(v_2(s, l_*))ds$$

$$\leq \frac{1}{2}|\mathbf{v}_0|_H^2 + C(p') \int_0^t \|\mathbf{u}\|_W^2 ds + C(p)\|\mathbf{u}(t)\|_W^2$$

$$+ \int_0^t \int_0^{l_*} R_m(u_{1x} + \Phi_x) \, dx \, ds + C.$$

The two terms involving Λ taken together are nonnegative. In fact, they equal

$$S(u_1(t, l_*) - u_2(t, l_*)),$$

where

$$S(r) = \int_0^r \Lambda(s)ds.$$

Then, by using Gronwall's inequality to eliminate the term

$$\int_0^t \int_0^{l_*} R_m(u_{1x} + \Phi_x) \, dx \, ds,$$

on the right-hand side, we can adjust the constants and obtain

$$|\mathbf{v}(t)|_H^2 + \min(d_1, d_2) \int_0^t \|\mathbf{v}(s)\|_V^2 ds + \min(k_1, k_2)\|\mathbf{u}(t)\|_V^2$$

$$+ \delta \int_0^{l_*} R_m(u_{1x}(t) + \Phi_x(t)) dx + \delta \int_{l_*}^1 R_m(u_{2x}(t)) dx + S(u_1(t, l_*) - u_2(t, l_*))$$

$$\leq C\Big(|\mathbf{v}_0|_H^2 + \int_0^t \|\mathbf{u}\|_W^2 ds + \|\mathbf{u}(t)\|_W^2 + 1\Big).$$

The two terms involving R_m are nonnegative, since R_m is nonnegative. Therefore, discarding these two terms yields

$$|\mathbf{v}(t)|_H^2 + \min(d_1, d_2) \int_0^t \|\mathbf{v}(s)\|_V^2 ds$$

$$+ \min(k_1, k_2)\|\mathbf{u}(t)\|_V^2 + S(u_1(t, l_*) - u_2(t, l_*))$$

$$\leq C\Big(|\mathbf{v}_0|_H^2 + \int_0^t \|\mathbf{u}\|_W^2 ds + \|\mathbf{u}(t)\|_W^2 + 1\Big).$$

The compactness of the embedding of V into W implies

$$|\mathbf{v}(t)|_H^2 + \min(d_1, d_2) \int_0^t \|\mathbf{v}(s)\|_V^2 ds$$

$$+ \min(k_1, k_2)\|\mathbf{u}(t)\|_V^2 + S(u_1(t, l_*) - u_2(t, l_*))$$

$$\leq C\Big(|\mathbf{v}_0|_H^2 + \int_0^t \|\mathbf{u}\|_W^2 ds + 1\Big) + \frac{1}{2}\min(k_1, k_2)\|\mathbf{u}(t)\|_V^2 + C|\mathbf{u}(t)|_H^2.$$

Also,

$$|\mathbf{u}(t)|_H^2 \leq C\Big(|\mathbf{u}_0|^2 + \int_0^t |\mathbf{v}(s)|^2 ds\Big),$$

and so an application of the Gronwall inequality yields

$$|\mathbf{v}(t)|_H^2 + \min(d_1, d_2) \int_0^t \|\mathbf{v}(s)\|_V^2 ds$$

$$+ S(u_1(t, l_*) - u_2(t, l_*)) + \min(k_1, k_2)\|\mathbf{u}(t)\|_V^2 \tag{4.13}$$

$$\leq C(\Phi, u_0, v_0, T, p_0, k_1, k_2).$$

It follows from the continuity of the embedding of H^1 into $C([0,1])$ that this estimate provides an upper bound on the values of $|u_{ix}(x, t)|$ that is independent of m. Therefore, by taking m sufficiently large, we find that the values of u_{ix} and $u_{1x}(t) + \Phi_x(t)$ remain in the unmodified region in the definition of Q_m in (4.2). This observation completes the proof of the following abstract version of Theorem 3.1.

Theorem 4.3. *Let* (A1)–(A5) *hold. Then, for each pair* (λ_1, λ_2) *there exists a unique solution* $(\mathbf{u}, \mathbf{v})$ *to*

$$\mathbf{v}' + A\mathbf{v} + B\mathbf{u} + N(\cdot, \mathbf{u}) + \pi_1^* \gamma^* \Lambda(u_1(l_*) - u_2(l_*))$$

$$- \pi_2^* \gamma^* \Lambda(u_1(l_*) - u_2(l_*)) = \mathbf{f}, \tag{4.14}$$

$$\mathbf{v}(0) = \mathbf{v}_0, \tag{4.15}$$

$$\mathbf{u}(t) = \mathbf{u}_0 + \int_0^t \mathbf{v}(s)ds. \tag{4.16}$$

This solution satisfies the estimate

$$\begin{aligned}
|\mathbf{v}(t)|_H^2 + \min(d_1, d_2) \int_0^t \|\mathbf{v}(s)\|_V^2 ds + \|\mathbf{u}(t)\|_V^2 \\
+ \int_0^{l_*} u_{1x}^4(t)\, dx + \int_{l_*}^1 u_{2x}^4(t)\, dx + S(u_1(t, l_*) - u_2(t, l_*)) \\
\le C(p_0, u_0, v_0, C_0, k_1, k_2, T),
\end{aligned} \tag{4.17}$$

where the constant on the right depends on the indicated quantities but is independent of $\lambda_1, \lambda_2, d_1$, and d_2.

The estimate follows directly from (4.13) and the continuity of the embedding of $H^1(I)$ into $C(I)$ when I is an interval. The continuity of this embedding implies that the solution to the truncated problem is such that u_{1x} and u_{2x} remain in the region where the truncation is inactive, thus yielding the unique solution in the theorem. This proves Theorem 3.1 as well.

5. The problem with the Signorini condition

We turn to the idealized problem with perfectly rigid stops, and use the results of the previous section. Indeed, we obtain a weak solution for the problem with the Signorini contact condition as a limit of the solutions of the problem with normal compliance in the limit when the normal compliance stiffness coefficients tend to infinity. Therefore, in this section we replace the coefficients with

$$\lambda_1 = \lambda_2 = n, \tag{5.1}$$

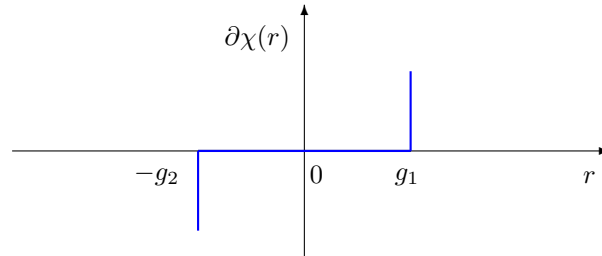and obtain the necessary a priori estimates to pass to the limit as $n \to \infty$.

Figure 5.1: The Signorini graph $\partial\chi(r)$, $r = 0$ corresponds to the center at $u_2(l_*, t)$

We have that the graph $\partial\chi(r)$, depicted in Figure 5.1, can be obtained from the graph of Λ in Figure 4.1 in the limit $n \to \infty$.

For the sake of convenience we will assume in this section that

$$u_{0ixx} \in L^\infty(I_i), \quad i = 1, 2.$$

Now, we recall the Signorini condition (2.13)-(2.14),

$$-g_2 \le u_1 - u_2 \le g_1,$$

$$\sigma(t) = \sigma_1(l_*, t) = -\sigma_2(l_*, t) \in \partial\chi(u_1(l_*, t) - u_2(l_*, t)).$$

We note that assumption (A1) implies that $\chi(u_{10}(l_*) - u_{20}(l_*)) = 0$.

We now add a subscript n to the solution to the problem with the normal compliance condition obtained in Section 4 that corresponds to the stiffnesses (5.1), so we denote the solutions of (4.14)–(4.16) as $(\mathbf{u}_n, \mathbf{v}_n)$.

We use below the following important theorem found in [40].

Theorem 5.1. *Let $q > 1$ and let $E \subseteq W \subseteq X$, where the injection map from W to X is continuous and is compact from E to W. Let S_R be defined by*

$$S_R = \big\{ u : \|u(t)\|_E + \|u'\|_{L^q([a,b];X)} \leq R, \ t \in [a,b] \big\}.$$

Then, $S_R \subseteq C([a,b]; W)$ and if $\{u_n\} \subseteq S_R$, there exists a subsequence, $\{u_{n_k}\}$ that converges uniformly to a function $u \in C([a,b]; W)$.

It follows from the theorem and estimate (4.17) that there exists a subsequence, still denoted as $\mathbf{u}_n$, such that as $n \to \infty$ the following convergences are obtained.

$$u_{inx} \to u_{ix} \quad \text{strongly in } C([0,T]; C(I_i)), \tag{5.2}$$

where here and below $I_1 = [0, l_*], I_2 = [l_*, 1]$, and $i = 1, 2$.

$$u_{ni} \to u_i \quad \text{strongly in } C([0,T]; C(I_i)), \tag{5.3}$$

$$\mathbf{u}_n \to \mathbf{u} \quad \text{weak} * \text{ in } L^\infty(0,T; V), \tag{5.4}$$

$$\mathbf{v}_n \to \mathbf{v} \quad \text{weakly in } \mathcal{V}, \tag{5.5}$$

$$\mathbf{v}_n \to \mathbf{v} \quad \text{weak} * \text{ in } L^\infty(0,T; H). \tag{5.6}$$

Next, let Λ_n be the function (2.9) with an obvious subscript, then it follows from the bound in (4.17) that

$$S_n(u_{1n}(l_*, t) - u_{2n}(l_*, t)) \leq C,$$

where C is independent of n, and so in the limit it follows from (5.3) that

$$-g_2 \leq (u_1(l_*, t) - u_2(l_*, t)) \leq g_1.$$

Therefore, $\mathbf{u} \in \mathcal{K}$ and so it satisfies the necessary constraint.

It follows from the equations estimate (5.2), that v_i' is bounded in

$$L^2\Big(0, T; (H_0^2(I_i))'\Big).$$

More precisely, we mean $i^* v_{in}'$ is bounded, where $i : H_0^2 \to V_0$ is the inclusion map. Therefore, we can also assume that

$$v_{ni}' \to v' \quad \text{in } L^2(0,T; (H_0^2(I_i))'). \tag{5.7}$$

To continue, we need the following fundamental theorem in [30].

Theorem 5.2. *Let $E \subseteq W \subseteq X$, where the injection map $i : W \to X$ is continuous and is compact from E to W. Let $p \geq 1$, let $q > 1$, and define*

$$S \equiv \big\{ u \in L^p([a,b]; E) : u' \in L^q([a,b]; X) \ \text{and}$$

$$\|u\|_{L^p([a,b];E)} + \|u'\|_{L^q([a,b];X)} \leq R \big\}.$$

Then, S is precompact in $L^p([a,b]; W)$, hence, if $\{u_n\}_{n=1}^\infty \subseteq S$, it has a subsequence $\{u_{n_k}\}$ which converges in $L^p([a,b]; W)$.

We apply this theorem to the case where $W = H_i$ and $E = V_i$ and find that addition to the above convergences, we also have

$$v_{ni} \to v_i \quad \text{strongly in } \mathcal{H}_i, \tag{5.8}$$

for a suitable subsequence. We let

$$V_0 = \{\mathbf{u} = (u_1, u_2) \in V : u_i \in H_0^2(I_i)\ i = 1, 2\},$$

and let $\mathcal{V}_0 = L^2((0, T); V_0)$. Then, it follows from the definition of the operators in (4.14) and the estimates above, that the expression

$$u_{n1tt} + d_1 v_{n1xxxx} + k_1 u_{n1xxxx} - \frac{1}{3}a_1((u_{n1x} + \Phi_x)^3)_x + \overline{\nu}_1 p u_{n1xx} + \Psi_{xx} \tag{5.9}$$

is bounded in $\mathcal{H}_1$, independently of n. Here, we use the appropriate measurable representatives so that the result is product measurable. It is obtained by applying the expression to $(\varphi, 0)$, where $\varphi \in C_0^\infty([0, T] \times [0, l_*])$, and using the density of the functions φ in $\mathcal{H}_1$. Similarly, we find that the expression

$$u_{n2tt} + d_2 v_{n2xxxx} + k_2 u_{n2xxxx} - \frac{1}{3}a_2((u_{n2x})^3 - \nu_2 p u_{n2x})_x \tag{5.10}$$

is bounded in $\mathcal{H}_2$, independently of n.

Because of the strong convergence in (5.2) - (5.6), there exists a further subsequence, still indexed by n, such that, in addition to (5.2) - (5.6), it also follows that the expression in (5.9) converges weakly in $\mathcal{H}_1$ to

$$m(x, t) \equiv u_{1tt} + d_1 v_{1xxxx} + k_1 u_{1xxxx} - \frac{1}{3}a_1((u_{1x} + \Phi_x)^3)_x + \overline{\nu}_1 p u_{1xx} + \Psi_{xx}, \tag{5.11}$$

and the expression in (5.10) converges weakly in $\mathcal{H}_1$ to

$$u_{2tt} + d_2 v_{2xxxx} + k_2 u_{2xxxx} - (\frac{a_2}{3}(u_{2x})^3 - \overline{\nu}_2 p u_{2x})_x. \tag{5.12}$$

Now, let $\psi \in W_0^{2,\infty}(I_1), \varphi \in W_0^{1,\infty}(0, T)$ and consider

$$\int_{I_1} \int_0^T m(x, t) u_1(x, t) \psi(x) \varphi(t)\, dt\, dx \tag{5.13}$$

$$= \int_{I_1} \int_0^T \left(-u_{1t}^2 + d_1 v_{1xx} u_{1xx} + k_1 u_{1xx}^2 \right.$$

$$\left. + \frac{a_1}{3}(u_{1x} + \Phi_x)^3 u_{1x} \right) \psi(x) \varphi(t) s\, dt\, dx \tag{5.14}$$

$$+ \int_{I_1} \int_0^T (-\overline{\nu}_1 p u_{1x}^2 - \Psi_x u_{1x}) \psi(x) \varphi(t)\, dt\, dx \tag{5.15}$$

$$+ \int_{I_1} \int_0^T (-u_{1t} \varphi'(t) \psi(x) u_1 + d_1 v_{1xx} \psi_{xx}(x) \varphi(t) u_1)\, dt\, dx \tag{5.16}$$

$$+ \int_{I_1} \int_0^T \left(k_1 u_{1xx} \psi_{xx}(x) \phi(t) u_1 + \frac{1}{3}a_1(u_{1x} + \Phi_x)^3 \psi_x(x) \phi(t) u_1 \right) dt\, dx \tag{5.17}$$

$$- \int_{I_1} \int_0^T (\overline{\nu}_1 p u_{1x} \psi_x(x) \phi(t) u_1 + \Phi_x \psi_x(x) \phi(t) u_1)\, dt\, dx. \tag{5.18}$$

We proceed in a similar way and obtain the analogous expression for the solutions that depend on n, so we replace u_1 with u_{n1} and v_1 with v_{n1} in (5.13)–(5.18). We

also replace $m(x,t)$ with $m_n(x,t)$. We obtain,

$$\int_{I_1} \int_0^T m_n(x,t)u_{n1}(x,t)\psi(x)\varphi(t)\,dt\,dx \tag{5.19}$$

$$= \int_{I_1} \int_0^T \left(-u_{n1t}^2 + d_1 v_{n1xx} u_{n1xx} + k_1 u_{n1xx}^2 \right.$$

$$\left. + \frac{1}{3} a_1 (u_{n1x} + \Phi_x)^3 u_{n1x} \right) \psi(x)\varphi(t)\,dt\,dx \tag{5.20}$$

$$+ \int_{I_1} \int_0^T (-\bar{\nu}_1 p u_{n1x}^2 - \Psi_x u_{n1x})\psi(x)\varphi(t)\,dt\,dx \tag{5.21}$$

$$+ \int_{I_1} \int_0^T (-u_{n1t}\varphi'(t)\psi(x)u_{n1} + d_1 v_{n1xx}\psi_{xx}(x)\varphi(t)u_{n1})\,dt\,dx$$

$$+ \int_{I_1} \int_0^T (k_1 u_{n1xx}\psi_{xx}(x)\varphi(t)u_{n1} + \frac{1}{3}a_1(u_{n1x} + \Phi_x)^3\psi_x(x)\varphi(t)u_{n1})\,dt\,dx$$

$$- \int_{I_1} \int_0^T (\bar{\nu}_1 p u_{n1x}\psi_x(x)\varphi(t)u_{n1} + \Psi_x\psi_x(x)\varphi(t)u_{n1})\,dt\,dx. \tag{5.22}$$

Then, the convergences established above imply that m_n converges weakly to m in $\mathcal{H}_1$ as $n \to \infty$. Indeed, (5.19) converges to (5.13) and the part between (5.21) - (5.22) converges to (5.15) - (5.18), and the part between (5.20) - (5.21) converges to (5.14) - (5.15). This is summarized as the following lemma.

Lemma 5.3. Let $\psi \in W_0^{2,\infty}(I_1), \phi \in W_0^{1,\infty}(0,T)$, then

$$\lim_{n\to\infty} \int_{I_1} \int_0^T \left(-u_{n1t}^2 + d_1 v_{n1xx} u_{n1xx} + k_1 u_{n1xx}^2 \right.$$

$$\left. + \frac{1}{3} a_1 (u_{n1x} + \Phi_x)^3 u_{n1x} \right) \psi\phi\,dt\,dx$$

$$+ \int_{I_1} \int_0^T (-\bar{\nu}_1 p u_{n1x}^2 - \Psi_x u_{n1x})\psi\phi\,dt\,dx$$

$$= \int_{I_1} \int_0^T \left(-u_{1t}^2 + d_1 v_{1xx} u_{1xx} + k_1 u_{1xx}^2 + \frac{1}{3} a_1 (u_{1x} + \Phi_x)^3 u_{1x} \right) \psi\phi\,dt\,dx$$

$$+ \int_{I_1} \int_0^T (-\bar{\nu}_1 p u_{1x}^2 - \Psi_x u_{1x})\psi\phi\,dt\,dx.$$

We claim that the above estimate holds without the product $\psi\phi$. To show this, we let φ_δ be a piecewise linear function such that $\varphi_\delta(0) = \varphi_\delta(T) = 0$, and $\varphi_\delta(t) = 1$ for $t \in [\delta, T-\delta]$, and let $\psi_\delta \in W_0^{2,\infty}(I_1)$ be a function such that $\psi_\delta(0) = \psi_\delta(1) = 0$, and $\psi_\delta(x) = 1$ for $x \in [\delta^2, l_* - \delta^2]$, with both ψ_δ and ϕ_δ having values in $[0,1]$. Then, we have the following lemma.

Lemma 5.4. The following estimate holds,

$$\limsup_{n\to\infty} \int_{I_1} \int_0^T \left(u_{n1t}^2 - d_1 v_{n1xx} u_{n1xx} - k_1 u_{n1xx}^2 - \frac{1}{3} a_1 (u_{n1x} + \Phi_x)^3 u_{n1x} \right) dt\,dx$$

$$+ \int_{I_1} \int_0^T (\bar{\nu}_1 p u_{n1x}^2 + \Psi_x u_{n1x})\,dt\,dx$$

$$\leq \int_{I_1} \int_0^T \left(u_{1t}^2 - d_1 v_{1xx} u_{1xx} - k_1 u_{1xx}^2 - \frac{1}{3} a_1 (u_{1x} + \Phi_x)^3 u_{1x} \right) dt\, dx$$

$$+ \int_{I_1} \int_0^T (\bar{\nu}_1 p u_{1x}^2 + \Psi_x u_{1x})\, dt\, dx.$$

Proof. Let ϕ_δ and ψ_δ be the functions described above. We denote by $Q_\delta = I_1 \setminus [\psi_\delta = 1]$, and assume that

$$\text{meas}(Q_\delta) < \delta,$$

and that δ is small enough so that if $\eta > 0$ is given then the following estimate is valid:

$$\frac{d_1}{2\delta} \int_{I_1} u_{01xx}^2 (1 - \psi_\delta) dx < \eta. \tag{5.23}$$

This is easily obtained because of the assumption that $u_{01xx} \in L^\infty$ and by the construction, $1 - \psi_\delta = 0$ off a set of measure $2\delta^2$. Also, let δ be small enough so that

$$\int_{I_1} \int_0^T v_1^2 (1 - \psi_\delta \phi_\delta)\, dt\, dx < \eta. \tag{5.24}$$

Next, consider the following integrals

$$J_{11} \equiv \int_{I_1} \int_0^T v_{n1}^2 (1 - \psi_\delta \phi_\delta)\, dt\, dx, \tag{5.25}$$

$$J_{12} \equiv \int_{I_1} \int_0^T -d_1 v_{n1xx} u_{n1xx} (1 - \psi_\delta \phi_\delta)\, dt\, dx, \tag{5.26}$$

$$J_{13} \equiv \int_{I_1} \int_0^T -k_1 u_{n1xx}^2 (1 - \psi_\delta \phi_\delta)\, dt\, dx. \tag{5.27}$$

First, we note that it follows from (5.24) and the strong convergence result in (5.8), that if n is sufficiently large, then

$$\int_{I_1} \int_0^T v_{n1}^2 (1 - \psi_\delta \phi_\delta)\, dt\, dx < \eta.$$

Below, we only consider such n. Next, we consider (5.27) and find

$$\limsup_{n \to \infty} \int_{I_1} \int_0^T -k_1 u_{n1xx}^2 (1 - \psi_\delta \phi_\delta)\, dt\, dx < \eta$$

It remains to consider (5.26), which is of the form

$$-\frac{1}{2} d_1 \int_{I_1} \int_0^T \frac{d}{dt}(u_{n1xx}^2)(1 - \psi_\delta \phi_\delta)\, dt\, dx.$$

We integrate this by parts and obtain

$$-\frac{1}{2} d_1 \int_{I_1} \left(u_{n1xx}^2 (1 - \psi_\delta \phi_\delta)|_0^T - \int_0^T u_{n1xx}^2 (-\psi_\delta \phi_\delta')dt \right) dx$$

$$= -\frac{1}{2} d_1 \left(\int_{I_1} u_{n1xx}^2(T)dx - \int_{I_1} u_{01xx}^2 + \int_{I_1} \int_0^T u_{n1xx}^2 \psi_\delta \phi_\delta' \right) dt\, dx$$

$$= -\frac{d_1}{2} \int_{I_1} u_{n1xx}^2(T)dx + \frac{d_1}{2} \int_{I_1} u_{01xx}^2 dx$$

$$-\frac{d_1}{2\delta}\int_{I_1}\int_0^\delta u_{n1xx}^2\psi_\delta\, dt\, dx + \frac{d_1}{2\delta}\int_{I_1}\int_{T-\delta}^T u_{n1xx}^2\psi_\delta\, dt\, dx$$

$$\leq \frac{d_1}{2\delta}\int_{I_1}\int_{T-\delta}^T (u_{n1xx}^2 - u_{n1xx}^2(T))\, dt\, dx + \frac{d_1}{2\delta}\int_{I_1}\int_0^\delta (u_{01xx}^2 - u_{n1xx}^2\psi_\delta)\, dt\, dx$$

$$= \frac{d_1}{2\delta}\int_{I_1}\int_{T-\delta}^T (u_{n1xx}^2 - u_{n1xx}^2(T))\, dt\, dx + \frac{d_1}{2\delta}\int_{I_1}\int_0^\delta (u_{01xx}^2 - u_{n1xx}^2)\psi_\delta\, dt\, dx$$

$$+ \frac{d_1}{2\delta}\int_{I_1}\int_0^\delta u_{01xx}^2(1 - \psi_\delta)\, dt\, dx$$

and (5.23) implies

$$\leq \frac{d_1}{2\delta}\int_{I_1}\int_{T-\delta}^T (u_{n1xx}^2 - u_{n1xx}^2(T))\, dt\, dx + \frac{d_1}{2\delta}\int_{I_1}\int_0^\delta (u_{01xx}^2 - u_{n1xx}^2)\psi_\delta\, dt\, dx + \eta l_*.$$
(5.28)

Now, the second term in (5.28) is dominated by

$$\frac{d_1}{2\delta}\int_{I_1}\int_0^\delta |(u_{01xx}^2 - u_{n1xx}^2)|\, dt\, dx$$

$$\leq \frac{d_1}{\delta}\int_{I_1}\int_0^\delta\int_0^t |v_{n1xx}u_{n1xx}|ds\, dt\, dx,$$

$$\leq \frac{d_1}{\delta}\int_0^\delta\int_{I_1}\int_0^\delta |v_{n1xx}(x,s)u_{n1xx}(x,s)|\, ds\, dx\, dt$$

$$\leq d_1\Big(\int_{I_1}\int_0^\delta |v_{n1xx}(x,s)|^2 ds dx\Big)^{1/2}\Big(\int_0^\delta\int_{I_1} |u_{n1xx}(x,s)|^2\, dx\, ds\Big)^{1/2}$$

$$\leq Cd_1\sqrt{\delta}\equiv C\sqrt{\delta},$$

thanks to estimate (4.17). Similar considerations apply to the first term of (5.28). Therefore, if δ is small enough, J_{12} in (5.26) is no larger than $\eta(1+l_*)$. We assume below that δ is this small.

Next, recall the strong convergence results on the lower order terms in (5.2). It follows that

$$\limsup_{n\to\infty}\int_{I_1}\int_0^T\Big(u_{n1t}^2 - d_1v_{n1xx}u_{n1xx} - k_1u_{n1xx}^2 - \frac{1}{3}a_1(u_{n1x}+\Phi_x)^3 u_{n1x}\Big)\, dt\, dx$$

$$+ \int_{I_1}\int_0^T (\bar{\nu}_1 p u_{n1x}^2 + \Psi_x u_{n1x})\, dt\, dx$$

$$\leq \limsup_{n\to\infty}\int_{I_1}\int_0^T (u_{n1t}^2 - d_1v_{n1xx}u_{n1xx} - k_1u_{n1xx}^2)\psi_\delta\phi_\delta\, dt\, dx$$

$$- \lim_{n\to\infty}\frac{1}{3}a_1\int_{I_1}\int_0^T (u_{n1x}+\Phi_x)^3 u_{n1x}\, dt\, dx$$

$$+ \lim_{n\to\infty}\int_{I_1}\int_0^T (\bar{\nu}_1 p u_{n1x}^2 + \Psi_x u_{n1x})\, dt\, dx$$

$$+ \limsup_{n\to\infty}\int_{I_1}\int_0^T (u_{n1t}^2 - d_1v_{n1xx}u_{n1xx} - k_1u_{n1xx}^2)(1 - \psi_\delta\phi_\delta)\, dt\, dx.$$

Now, by Lemma 5.3 and the above estimates on the integrals (5.25) - (5.27), we find

$$\limsup_{n\to\infty} \int_{I_1} \int_0^T \left(u_{n1t}^2 - d_1 v_{n1xx} u_{n1xx} - k_1 u_{n1xx}^2 - \frac{1}{3} a_1 (u_{n1x} + \Phi_x)^3 u_{n1x} \right) dt\, dx$$

$$+ \int_{I_1} \int_0^T (\bar{\nu}_1 p u_{n1x}^2 + \Psi_x u_{n1x})\, dt\, dx$$

$$\leq \int_{I_1} \int_0^T (u_{1t}^2 - d_1 v_{1xx} u_{1xx} - k_1 u_{1xx}^2) \psi_\delta \phi_\delta\, dt\, dx$$

$$- \frac{1}{3} a_1 \int_{I_1} \int_0^T ((u_{1x} + \Phi_x)^3 u_{1x})\, dt\, dx$$

$$+ \int_{I_1} \int_0^T (\bar{\nu}_1 p u_{1x}^2 + \Psi_x u_{1x})\, dt\, dx + (3 + l_*)\eta$$

since $u_{1t}^2 - d_1 v_{1xx} u_{1xx} - k_1 u_{1xx}^2$ is in L^1, this implies that for δ possibly even smaller,

$$\leq \int_{I_1} \int_0^T (u_{1t}^2 - d_1 v_{1xx} u_{1xx} - k_1 u_{1xx}^2)\, dt\, dx - \frac{1}{3} a_1 \int_{I_1} \int_0^T ((u_{1x} + \Phi_x)^3 u_{1x})\, dt\, dx$$

$$+ \int_{I_1} \int_0^T (\bar{\nu}_1 p u_{1x}^2 + \Psi_x u_{1x})\, dt\, dx + (4 + l_*)\eta.$$

Since η is arbitrary, this establishes the lemma. $\qquad\square$

The same arguments establish the following lemma.

Lemma 5.5. *The following estimate holds,*

$$\limsup_{n\to\infty} \int_{I_2} \int_0^T (u_{n2t}^2 - d_2 v_{n2xx} u_{n2xx} - k_1 u_{n2xx}^2 - \frac{a_2}{3}(u_{n2x})^4)\, dt\, dx$$

$$+ \int_{I_2} \int_0^T \bar{\nu}_2 p u_{n2x}^2\, dt\, dx$$

$$\leq \int_{I_2} \int_0^T (u_{2t}^2 - d_2 v_{2xx} u_{2xx} - k_1 u_{2xx}^2 - \frac{a_2}{3}(u_{2x})^4)\, dt\, dx + \int_{I_2} \int_0^T \bar{\nu}_2 p u_{2x}^2\, dt\, dx.$$

Lemmas 5.4 and 5.4 imply the following two inequalities.

$$\liminf_{n\to\infty} \int_{I_2} \int_0^T (-u_{n2t}^2 + d_2 v_{n2xx} u_{n2xx} + k_1 u_{n2xx}^2 + \frac{a_2}{3}(u_{n2x})^4)\, dt\, dx$$

$$- \int_{I_2} \int_0^T \bar{\nu}_2 p u_{n2x}^2\, dt\, dx$$

$$\geq \int_{I_2} \int_0^T (-u_{2t}^2 + d_2 v_{2xx} u_{2xx} + k_1 u_{2xx}^2 + \frac{a_2}{3}(u_{2x})^4)\, dt\, dx$$

$$- \int_{I_2} \int_0^T \bar{\nu}_2 p u_{2x}^2\, dt\, dx,$$

(5.29)

and

$$\liminf_{n \to \infty} \int_{I_1} \int_0^T \left(-u_{n1t}^2 + d_1 v_{n1xx} u_{n1xx} + k_1 u_{n1xx}^2 + \frac{1}{3} a_1 (u_{n1x} + \Phi_x)^3 u_{n1x} \right) dt\, dx$$

$$- \int_{I_1} \int_0^T (\bar{\nu}_1 p u_{n1x}^2 + \Psi_x u_{n1x})\, dt\, dx$$

$$\geq \int_{I_1} \int_0^T \left(-u_{1t}^2 + d_1 v_{1xx} u_{1xx} + k_1 u_{1xx}^2 + \frac{a_1}{3}(u_{1x} + \Phi_x)^3 u_{1x} \right) dt\, dx$$

$$- \int_{I_1} \int_0^T (\bar{\nu}_1 p u_{1x}^2 + \Psi_x u_{1x})\, dt\, dx. \tag{5.30}$$

Now, we define Λ_n as

$$\Lambda_n(u_{n1}(l_*, t) - u_{n2}(l_*, t))$$
$$\equiv -n(u_{n1}(l_*, t) - u_{n2}(l_*, t) - g_1)_+ + n(u_{n2}(l_*, t) - u_{n1}(l_*, t) - g_2)_+, \tag{5.31}$$

and the two operators

$$P_n(\mathbf{u}_n) \equiv \pi_1^* \gamma^* \Lambda_n(u_{n1}(l_*, t) - u_{n2}(l_*, t)) - \pi_2^* \gamma^* \Lambda_n(u_1(l_*, t) - u_2(l_*, t)),$$
$$P(\mathbf{u}) \equiv \pi_1^* \gamma^* \partial \chi(u_1(l_*, t) - u_2(l_*, t)) - \pi_2^* \gamma^* \partial \chi(u_1(l_*, t) - u_2(l_*, t)).$$

As was noted above, these operators are monotone because of the graph of Λ_n. Also, the solution of the problem with normal compliance satisfies

$$\mathbf{v}_n' + A\mathbf{v}_n + B\mathbf{u}_n + N(\cdot, \mathbf{u}_n) + P_n(\mathbf{u}_n) = \mathbf{f}, \tag{5.32}$$

together with $\mathbf{v}_n(0) = \mathbf{v}_0$ and $\mathbf{u}_n(t) = \mathbf{u}_0 + \int_0^t \mathbf{v}_n(s) ds$. It was shown above that

$$-g_2 \leq u_1(l_*, t) - u_2(l_*, t) \leq g_1.$$

Inequalities (5.29) - (5.30) can be written simply in terms of the operators as

$$\liminf_{n \to \infty} \left(-\int_0^T (\mathbf{v}_n, \mathbf{v}_n)_H dt + \int_0^T \langle A\mathbf{v}_n, \mathbf{u}_n \rangle dt \right.$$

$$+ \int_0^T \langle B\mathbf{u}_n, \mathbf{u}_n \rangle dt + \int_0^T \langle N(\cdot, \mathbf{u}_n), \mathbf{u}_n \rangle dt \Big)$$

$$\geq \left(-\int_0^T (\mathbf{v}, \mathbf{v})_H dt + \int_0^T \langle A\mathbf{v}, \mathbf{u} \rangle dt + \int_0^T \langle B\mathbf{u}, \mathbf{u} \rangle dt + \int_0^T \langle N(\cdot, \mathbf{u}), \mathbf{u} \rangle dt \right). \tag{5.33}$$

Here, we used the notation $\langle \cdot, \cdot \rangle$ for the duality pairing between V and V'.

Now, let $\mathbf{w}, \mathbf{w}' \in \mathcal{V}$ such that $\mathbf{w}(T) = \mathbf{u}(T)$ and for each t,

$$-g_2 \leq w_1(l_*, t) - w_2(l_*, t) \leq g_1.$$

We apply (5.32) to $\mathbf{u}_n - \mathbf{w}$ and perform time integration on both sides. Thus,

$$-\int_0^T (\mathbf{v}_n, \mathbf{v}_n - \mathbf{w}')dt + (\mathbf{v}_0, \mathbf{w}(0) - \mathbf{u}_0)_H + \int_0^T \langle A\mathbf{v}_n, \mathbf{u}_n - \mathbf{w} \rangle ds$$

$$+ \int_0^T \langle B\mathbf{u}_n, \mathbf{u}_n - \mathbf{w} \rangle ds + \int_0^T \langle N(\cdot, \mathbf{u}_n), \mathbf{u}_n - \mathbf{w} \rangle dt + \int_0^T \langle P_n(\mathbf{u}_n), \mathbf{u}_n - \mathbf{w} \rangle dt$$

$$= \int_0^T (\mathbf{f}, \mathbf{u}_n - \mathbf{w})_H ds.$$

Since $P_n(\mathbf{w}) = 0$, it follows that

$$\int_0^T \langle P_n(\mathbf{u}_n), \mathbf{u}_n - \mathbf{w}\rangle dt = \int_0^T \langle P_n(\mathbf{u}_n) - P_n(\mathbf{w}), \mathbf{u}_n - \mathbf{w}\rangle dt \geq 0;$$

therefore,

$$-\int_0^T (\mathbf{v}_n, \mathbf{v}_n - \mathbf{w}')dt + (\mathbf{v}_0, \mathbf{w}(0) - \mathbf{u}_0)_H + \int_0^T \langle A\mathbf{v}_n, \mathbf{u}_n - \mathbf{w}\rangle ds$$

$$+ \int_0^T \langle B\mathbf{u}_n, \mathbf{u}_n - \mathbf{w}\rangle ds + \int_0^T \langle N(\cdot, \mathbf{u}_n), \mathbf{u}_n - \mathbf{w}\rangle dt$$

$$\leq \int_0^T (\mathbf{f}, \mathbf{u}_n - \mathbf{w})_H ds.$$

Passing to the $\liminf_{n\to\infty}$ of both sides, it follows from (5.33) that

$$-\int_0^T (\mathbf{v}, \mathbf{v} - \mathbf{w}')dt + (\mathbf{v}_0, \mathbf{w}(0) - \mathbf{u}_0)_H + \int_0^T \langle A\mathbf{v}, \mathbf{u} - \mathbf{w}\rangle ds$$

$$+ \int_0^T \langle B\mathbf{u}, \mathbf{u} - \mathbf{w}\rangle ds + \int_0^T \langle N(\cdot, \mathbf{u}), \mathbf{u} - \mathbf{w}\rangle dt \tag{5.34}$$

$$\leq \int_0^T (\mathbf{f}, \mathbf{u} - \mathbf{w})_H ds.$$

This concludes the proof of Theorem 3.2, which we restate as:

Theorem 5.6. *Assume that* (A1)–(A5) *hold along with the regularity assumption on the initial data*

$$u_{0ixx} \in L^\infty(I_i).$$

Then, there exists a pair $(\mathbf{u}, \mathbf{v})$ *such that*

$$\mathbf{u}(t) = \mathbf{u}_0 + \int_0^t \mathbf{v}(s)ds,$$

$\mathbf{v} \in \mathcal{V}$, *and* $\mathbf{u}(t) \in \mathcal{K}$ *such that whenever* $\mathbf{w}(t) \in \mathcal{K}$ *with* $\mathbf{w}, \mathbf{w}' \in \mathcal{V}$, *and* $\mathbf{w}(T) = \mathbf{u}(T)$, *then the variational inequality* (5.34) *holds.*

6. The inviscid case

In this section we study the case with the Signorini contact condition when there is no viscosity, so, as above, we replace the normal compliance stiffness coefficients λ_1, λ_2 and the viscosity coefficients d_1, d_2 with the modified coefficients

$$n\lambda_1, \quad n\lambda_2, \quad \frac{d_1}{n}, \quad \frac{d_2}{n},$$

and consider a sequence of solutions, one for each positive integer n. Then, we obtain the necessary estimates and consider the limit when $n \to \infty$. The above discussion of the normal compliance case yields the following result.

Theorem 6.1. *Assume that* (A1)–(A5) *hold. Then, for each n there exists a unique solution to the abstract problem*

$$\mathbf{v}' + \frac{1}{n}A\mathbf{v} + B\mathbf{u} + N(\cdot, \mathbf{u}) + \pi_1^* \gamma^* n\Lambda(u_1(l_*) - u_2(l_*))$$
$$- \pi_2^* \gamma^* n\Lambda(u_1(l_*) - u_2(l_*)) = \mathbf{f}, \tag{6.1}$$

together with $\mathbf{v}(0) = \mathbf{v}_0$, *and* $\mathbf{u}(t) = \mathbf{u}_0 + \int_0^t \mathbf{v}(s)ds.$

This solution satisfies for a.e. $t \in (0, T)$ *the estimate*

$$
\begin{aligned}
&|\mathbf{v}(t)|_H^2 + \frac{1}{n} \min(d_1, d_2) \int_0^t \|\mathbf{v}(s)\|_V^2 ds + \int_0^{l_*} u_{1x}(t)^4 dx \\
&+ \int_{l_*}^1 u_{2x}(t)^4 dx + \|\mathbf{u}(t)\|_V^2 + nS(u_1(t, l_*) - u_2(t, l_*)) \\
&\le C(p_0, \mathbf{v}_0, \mathbf{u}_0, C_0, k_1, k_2, T)
\end{aligned}
\tag{6.2}
$$

where the constant C *depends on the indicated quantities but is independent of* n *and* d_i.

Estimate (6.2) yields the same type of convergence results that were obtained above, with the exception of (5.5), which is lost but is replaced with a related convergence. Specifically, we have

$$
\begin{aligned}
u_{inx} &\to u_{ix} \quad \text{strongly in } C([0, T]; C(I_i)), \\
u_{ni} &\to u_i \quad \text{strongly in } C([0, T]; C(I_i)), \\
\mathbf{u}_n &\to \mathbf{u} \quad \text{weak} * \text{ in } L^\infty(0, T; V) \\
\frac{1}{\sqrt{n}} &\mathbf{v}_{nxx} \to 0 \text{ strongly in } \mathcal{H}, \\
\mathbf{v}_n &\to \mathbf{v} \quad \text{weak} * \text{ in } L^\infty(0, T; H).
\end{aligned}
\tag{6.3}
$$

It follows from (6.2) and (6.3), as above, that

$$
-g_2 \le (u_1(t, l_*) - u_2(t, l_*)) \le g_1.
$$

Therefore, $\mathbf{u} \in \mathcal{K}$ and so it satisfies the necessary constraint.

Estimates (6.2) and (6.1) imply that, just as above, the function v_i' is bounded in $L^2(0, T; (H_0^2(I_i))')$. Therefore, we can also assume that

$$
v_{ni}' \to v' \text{ in } L^2\Big(0, T; (H_0^2(I_i))'\Big).
$$

Now, the rest of the argument is similar to the above except for the issue involving the viscous term. The formula (5.26) now takes the form

$$
-\frac{d_1}{n} \int_{I_1} \int_0^T v_{n1xx} u_{n1xx}(1 - \psi_\delta \phi_\delta) \, dt \, dx.
\tag{6.4}
$$

Then, all the same considerations hold in the argument for approximation. Consider next the integral

$$
\frac{1}{n} \int_{I_1} \int_0^T v_{n1xx} u_{n1xx} \, dt \, dx,
$$

which converges to 0 because of the estimate

$$
\begin{aligned}
&\Big| \frac{1}{n} \int_{I_1} \int_0^T v_{n1xx} u_{n1xx} \, dt \, dx \Big| \\
&\le \Big(\frac{1}{n^2} \int_{I_1} \int_0^T v_{nxx}^2 \, dt \, dx \Big)^{1/2} \Big(\int_{I_1} \int_0^T u_{n1xx}^2 \, dt \, dx \Big)^{1/2} \\
&\le \frac{1}{\sqrt{n}} \Big(\int_{I_1} \int_0^T \frac{1}{n} v_{nxx}^2 \, dt \, dx \Big)^{1/2} \Big(\int_{I_1} \int_0^T u_{n1xx}^2 \, dt \, dx \Big)^{1/2},
\end{aligned}
$$

which converges to 0 by the estimates derived above.

It follows that

$$\liminf_{n \to \infty} \Big(- \int_0^T (\mathbf{v}_n, \mathbf{v}_n)_H dt + \int_0^T \langle \frac{1}{n} A\mathbf{v}_n, \mathbf{u}_n \rangle dt$$

$$+ \int_0^T \langle B\mathbf{u}_n, \mathbf{u}_n \rangle dt + \int_0^T \langle N(\cdot, \mathbf{u}_n), \mathbf{u}_n \rangle dt \Big)$$

$$\geq \Big(- \int_0^T (\mathbf{v}, \mathbf{v})_H dt + \int_0^T \langle B\mathbf{u}, \mathbf{u} \rangle dt + \int_0^T \langle N(\cdot, \mathbf{u}), \mathbf{u} \rangle dt \Big),$$

so that the viscous term disappears. Then, the same argument as above yields the theorem for the inviscid case and with the Signorini contact condition.

Theorem 6.2. *Assume that* (A1)–(A5) *hold along with the regularity assumption on the initial data*

$$u_{0ixx} \in L^\infty(I_i).$$

Then, there exists a pair $\mathbf{u}, \mathbf{v} \in \mathcal{V}$, $\mathbf{u}(t) = \mathbf{u}_0 + \int_0^t \mathbf{v}(s)ds$, $\mathbf{u}(t) \in \mathcal{K}$ *such that whenever* $\mathbf{w}(t) \in \mathcal{K}$ *with* $\mathbf{w}' \in \mathcal{V}$, $\mathbf{w}(T) = \mathbf{u}(T)$, *it follows*

$$- \int_0^T (\mathbf{v}, \mathbf{v} - \mathbf{w}')_H dt + \int_0^T \langle B\mathbf{u}, \mathbf{u} - \mathbf{w} \rangle ds + \int_0^T \langle N(\cdot, \mathbf{u}), \mathbf{u} - \mathbf{w} \rangle dt$$

$$\leq \int_0^T (\mathbf{f}, \mathbf{u} - \mathbf{w})_H ds - (\mathbf{v}_0, \mathbf{w}(0) - \mathbf{u}_0)_H.$$

To obtain the existence result for the inviscid problem with normal compliance we replace the inequality with the following variational equation

$$- \int_0^T (\mathbf{v}, \mathbf{v} - \mathbf{w}')_H dt + \int_0^T \langle B\mathbf{u}, \mathbf{u} - \mathbf{w} \rangle ds + \int_0^T \langle N(\cdot, \mathbf{u}), \mathbf{u} - \mathbf{w} \rangle dt$$

$$+ \int_0^T \Lambda(u_1(t, l_*) - u_2(t, l_*))(w_1(t, l_*))dt$$

$$- \int_0^T \Lambda(u_1(t, l_*) - u_2(t, l_*))(w_2(t, l_*))dt$$

$$= \int_0^T (\mathbf{f}, \mathbf{u} - \mathbf{w})_H ds - (\mathbf{v}_0, \mathbf{w}(0) - \mathbf{u}_0)_H,$$

and note that the requirement that $\mathbf{u} \in \mathcal{K}$ is not needed.

This concludes the analysis part of this work. The rest of the paper deals with the numerical aspects of the model.

7. Computational method; numerical algorithm

In this section we describe our numerical schemes for the model. Unlike the Euler–Bernoulli or the Timoshenko beams, the two Gao beams are nonlinear, which makes the approach more complex.

We choose a fully discrete numerical method and use a uniform discretization of the time domain $[0, T]$ and a mixture of the Galerkin approximation and central difference formula to discretize the space domain $[0, 1]$. The central difference formula is combined with the finite element method (FEM) when we deal with the nonlinear Gao terms in the two equations. Convergence results of similar numerical schemes have been investigated in [4], using a modified truncated operator in the discrete case. We note that a different numerical algorithm for a Gao beam,

but without contact, was presented in [7], where the fully explicit finite difference method (FDM) was used.

Since the equation of a Gao beam contains second and fourth order derivatives, we use a nonconforming mixed finite element method. Indeed, nonconforming methods which have been studied in many papers and books (e.g., [13, 14] and the references therein) provide more efficient and practical algorithms for the fourth order or even higher order PDEs. The mixed method that yields a saddle-point problem has been first proposed in [36] and its convergence analysis has been studied extensively, see, e.g., [11, 12] and the references therein.

We now describe our numerical schemes. The interval $[0, 1]$ is divided into m subintervals $I_i = [x_i, x_{i+1}]$, for $0 \leq i \leq m - 1$, with grid points

$$0 = x_0 < x_1 < x_2 < \cdots < x_{i_*} < \cdots < x_{m-2} < x_{m-1} < x_m = 1.$$

For the sake of simplicity, a uniform spacing is used and the mesh size is denoted by $h_x = x_{i+1} - x_i$. We assume that the two beams are joined at the node $x = x_{i_*}$. According to the nonconforming finite element methods and Sobolev imbedding theorem, we choose V_{h_x} as the finite dimensional space

$$V_{h_x} = \{w_{h_x} \in C[0, 1] : w_{h_x}\big|_{I_i} \in \mathcal{L}(I_i) \cup \mathcal{B}(I_i), 1 \leq i \leq m - 1\},$$

where $\mathcal{L}$ is the family of piecewise linear functions and $\mathcal{B}$ is the family of the piecewise cubic functions. The finite element space can be written in the equivalent way

$$V_{h_x} = \text{span}\{\psi_i \in C[0, x_{i_*}] \cup C[x_{i_*}, 1] : 1 \leq i \leq m - 1\}.$$

The basis functions ψ_i are constructed next. We note that on the node x_{i_*} two different basis functions have to be constructed separately, since one is associated with the right end of the left beam and the other is with the left end of the right beam. We construct the basis functions $\psi_i = \psi_{1,i}$ with compact supports $[x_{i-1}, x_{i+1}]$ and $\psi_i = \psi_{3,i}$ with compact supports $[x_{i-2}, x_{i+2}]$; the first is a typical piecewise linear function $L(s)$ for the basis functions denoted by $\psi_{1,i} \in C[0, 1]$ and the other is a cubic spline functions $B(s)$ for the basis functions denoted by $\psi_{3,i} \in C^1[0, 1]$. It is easy to construct the piecewise linear functions on the reference interval $[-1, 1]$ and the standard cubic spline functions $B(s)$ on the reference interval $[-2, 2]$,

$$L(s) = \begin{cases} -|s| + 1 & \text{if } |s| \leq 1, \\ 0 & \text{if } |s| \geq 1, \end{cases}$$

and

$$B(s) = \frac{2}{3} \begin{cases} 1 + \frac{3}{4}|s|^3 - \frac{3}{2}|s|^2 & \text{for } |s| \leq 1, \\ \frac{1}{4}(2 - |s|)^3 & \text{for } 1 \leq |s| \leq 2, \\ 0 & \text{for } |s| \geq 2. \end{cases}$$

For the piecewise linear functions with $1 < i \leq m - 1$ the basis functions $\psi_{1,i}$ is defined by the shifted linear function

$$\psi_{1,i}(x) = L\big(\frac{x - x_i}{h_x}\big),$$

where each node is $x_i = i\, h_x$ and their supports are $[x_i - h_x, x_i + h_x]$. For the B-spline functions with $2 < i \leq i_* - 2$ and $i_* + 2 < i \leq m - 1$ we use mostly the basis functions $\psi_{3,i}$ defined by the shifted cubic splines

$$\psi_{3,i}(x) = B\big(\frac{x - x_i}{h_x}\big),$$

where each node is $x_i = i\, h_x$ and their supports are $[x_i - 2h_x,\, x_i + 2h_x]$. While it is not hard to set up the piecewise linear functions $\psi_{1,i}$ with the boundary conditions, we need to be more careful about constructing the basis functions $\psi_{3,i}$ so as to satisfy the boundary conditions. In order to satisfy all the conditions, the cubic functions are modified as follows:

$$\psi_{3,1}(x) = \begin{cases} -\frac{5}{3}(\frac{x}{h_x})^3 + \frac{5}{2}(\frac{x}{h_x})^2 & \text{on } [0,\, h_x], \\ \frac{5}{6}(\frac{x}{h_x} - 1)^3 - \frac{3}{2}(\frac{x}{h_x} - 1)^2 + \frac{5}{6} & \text{on } [h_x,\, 2h_x], \\ \frac{1}{6}(2 - (\frac{x}{h_x} - 1))^3 & \text{on } [2h_x,\, 3h_x], \end{cases}$$

and

$$\psi_{3,m-1}(x)$$
$$= \begin{cases} \frac{5}{3}(\frac{x}{h_x} - m)^3 + \frac{5}{2}(\frac{x}{h_x} - m)^2 & \text{on } [1 - h_x,\, 1], \\ -\frac{5}{6}(\frac{x}{h_x} - (m-1))^3 - \frac{3}{2}(\frac{x}{h_x} - (m-1))^2 + \frac{5}{6} & \text{on } [1 - 2h_x,\, 1 - h_x], \\ \frac{1}{6}(2 + (\frac{x}{h_x} - (m-1)))^3 & \text{on } [1 - 3h_x,\, 1 - 2h_x]. \end{cases}$$

We need to construct the two basis functions satisfying the natural boundary conditions imposed at $x = l_*$. The basis functions ψ_{i_*-1} and ψ_{i_*} are

$$\psi_{3,i_*-1}(x)$$
$$= \begin{cases} -\frac{5}{3}(\frac{x}{h_x} - (i_* - 1))^3 + \frac{5}{2}(\frac{x}{h_x} - (i_* - 1))^2 & \text{on } [x_{i_*} - h_x,\, x_{i_*}], \\ \frac{5}{6}(\frac{x}{h_x} - (i_* - 2))^3 - \frac{3}{2}(\frac{x}{h_x} - (i_* - 2))^2 + \frac{5}{6} & \text{on } [x_{i_*} - 2h_x,\, x_{i_*} - h_x], \\ \frac{1}{6}(2 - (\frac{x}{h_x} - (i_* - 2)))^3 & \text{on } [x_{i_*} - 3h_x,\, x_{i_*} - 2h_x], \end{cases}$$

and

$$\psi_{3,i_*}(x) = -\frac{2}{h_x^3}(x - (i_* - 1))^3 - \frac{3}{h_x^2}(x - (i_* - 1))^2 \quad \text{on } [x_{i_*} - h_x,\, x_{i_*}].$$

Similarly for the right Gao beam, we can obtain

$$\psi_{3,i_*}(x) = \frac{2}{h_x^3}(x - (i_* + 1))^3 + \frac{3}{h_x^2}(x - (i_* + 1))^2 \quad \text{on } [x_{i_*},\, x_{i_*} + h_x].$$

and

$$\psi_{3,i_*+1}(x)$$
$$= \begin{cases} -\frac{5}{3}(\frac{x}{h_x} - i_*)^3 + \frac{5}{2}(\frac{x}{h_x} - i_*)^2 & \text{on } [x_{i_*},\, x_{i_*} + h_x], \\ \frac{5}{6}(\frac{x}{h_x} - (i_* + 1))^3 - \frac{3}{2}(\frac{x}{h_x} - (i_* + 1))^2 + \frac{5}{6} & \text{on } [x_{i_*} + h_x,\, x_{i_*} + 2h_x], \\ -\frac{1}{6}(2 - (\frac{x}{h_x} - (i_* + 2)))^3 & \text{on } [x_{i_*} + 2h_x,\, x_{i_*} + 3h_x]. \end{cases}$$

The time interval $[0, T]$ is also uniformly partitioned as

$$0 = t_0 < t_1 < t_2 \cdots < t_k < \cdots < t_{n-1} < t_n = T,$$

where $h_t = t_k - t_{k-1}$, for $1 \le k \le n$. We suppose that at each time step $t = t_k$ the fully discrete solutions u_{1h_t,h_x}^k and u_{2h_t,h_x}^k are represented by linear combinations of B-splines over the domain $[0, 1]$ as

$$u_{1h_t,h_x}^k = \sum_{i=1}^{i_*} u_{1i}^k \psi_{d,i}(x), \quad u_{2h_t,h_x}^k = \sum_{i=i_*}^{m-1} u_{2i}^k \psi_{d,i}(x),$$

where d is the degree of the B-splines. When we deal with the 0th and 2nd order partial derivative with respect to x, we write the fully discrete solutions of the displacement and velocity as

$$u_{1h_t,h_x}^k = \sum_{i=1}^{i_*} u_{1i}^k \psi_{1,i}(x), \quad u_{2h_t,h_x}^k = \sum_{i=i_*}^{m-1} u_{2i}^k \psi_{1,i}(x),$$

$$(u_{1h_t,h_x}^k)_t = \sum_{i=1}^{i_*} v_{1i}^k \psi_{1,i}(x), \quad (u_{2h_t,h_x}^k)_t = \sum_{i=i_*}^{m-1} v_{2i}^k \psi_{1,i}(x). \tag{7.1}$$

Similarly, the solutions of the fourth-order partial derivative are

$$u_{1h_t,h_x}^k = \sum_{i=1}^{i_*} u_{1i}^k \psi_{3,i}(x), \quad u_{2h_t,h_x}^k = \sum_{i=i_*}^{m-1} u_{2i}^k \psi_{3,i}(x). \tag{7.2}$$

To derive the mixed method, we rewrite the original problem as the following mixed form,

$$\begin{bmatrix} u_{1tt} \\ \omega_1 \\ u_{2tt} \\ \omega_2 \end{bmatrix} = \begin{bmatrix} -k_1\omega_1 - d_1\omega_{1t} + a_1(u_{1x})^2 u_{1xx} - \bar{\nu}_1\, p(t)\, u_{1xx} + f_1(t) \\ u_{1xxxx} \\ -k_2\varpi_2 - d_2\varpi_{2t} + a_2(u_{2x})^2 u_{2xx} - \bar{\nu}_2\, p(t)\, u_{2xx} + f_2(t) \\ u_{2xxxx} \end{bmatrix}.$$

Multiplying each equation by a suitable test function and using integration by parts, it is straightforward to obtain the following weak formulation:

Find $(u_1, \omega_1, u_2, \omega_2) \in H^2(0, l_*) \times L^2(0, l_*) \times H^2(l_*, 1) \times L^2(l_*, 1)$ such that

$$0 = (u_{1tt} + k_1\omega_1 + d_1\omega_{1t} - a_1(u_{1x})^2 u_{1xx} + \bar{\nu}_1\, p(t)\, u_{1xx} - f_1(t),\, w)_{L^2(0, l_*)}$$
$$+ \sigma(t)\, w(l_*) \quad \text{for all } w \in L^2(0, l_*),$$

$$0 = (\omega_1,\, v)_{L^2(0, l_*)} - (u_{1xx},\, v_{xx})_{L^2(0, l_*)} \quad \text{for all } v \in H^2(0, l_*),$$

$$0 = \Big(u_{2tt} + k_2\varpi_2 + d_2\varpi_{2t} - a_2(u_{2x})^2 w_{2xx} + \bar{\nu}_2\, p(t)\, w_{2xx} - f_2(t),\, u\Big)_{L^2(l_*, 1)}$$
$$- \sigma(t)\, w(l_*) \quad \text{for all } u \in L^2(l_*, 1),$$

$$0 = (\omega_2,\, \mu)_{L^2(l_*, 1)} - (w_{2xx},\, \mu_{xx})_{L^2(l_*, 1)} \quad \text{for all } \mu \in H^2(l_*, 1),$$

where at $x = l_*$ we have $\sigma(t) = \sigma_1(t) = -\sigma_2(t)$. Then, the corresponding FEM can be applied easily. We assume that the auxiliary variables $\omega_1 = u_{1xxxx}$ and $\varpi_2 = u_{2xxxx}$ and $\omega_{1t} = u_{1txxxx}$ and $\varpi_{2t} = u_{2txxxx}$ are linear combinations of the piecewise constant functions $\psi_{0,i}$ with $1 \le i \le m-1$,

$$\omega_{1h_t,h_x}^k = \sum_{i=1}^{i_*} \omega_{1i}^k \psi_{0,i}(x), \quad \varpi_{2h_t,h_x}^k = \sum_{i=i_*}^{m-1} \omega_{2i}^k \psi_{0,i}(x),$$

$$(\omega_{1h_t,h_x}^k)_t = \sum_{i=1}^{i_*} \varpi_{1i}^k \psi_{0,i}(x), \quad (\omega_{2h_t,h_x}^k)_t = \sum_{i=i_*}^{m-1} \varpi_{2i}^k \psi_{0,i}(x) \quad \text{at } t = t_k.$$

When the weak formulation is written in the corresponding matrix form, the supports of the $\psi_{0,i}$ change, since when we deal with the B-spline of the degree $d = 0$, we use $\psi_{0,i}(x) = 1$ over $[x_{i-1}, x_{i+1}]$ and when we deal with cubic B-spline, we use

$\psi_{0,i}(x) = 1$ over $[x_{i-2}, x_{i+2}]$. In the discrete form, we obtain the following equation by using the test functions. Let

$$\boldsymbol{\omega}_{h_t,h_x}^k = (\omega_{1h_t,h_x}^k, \omega_{2h_t,h_x}^k)^T, \quad (\boldsymbol{\omega}_{h_t,h_x}^k)_t = (\varpi_{1h_t,h_x}^k, \varpi_{2h_t,h_x}^k)^T,$$
$$\mathbf{u}_{h_t,h_x}^k = (u_{1h_t,h_x}^k, u_{2h_t,h_x}^k)^T, \quad \mathbf{v}_{h_t,h_x}^k = (v_{1h_t,h_x}^k, v_{2h_t,h_x}^k)^T,$$

at each time step t_k. For the sake of simplicity, we assume that there are no body forces, i.e., $f_1 = f_2 = 0$. In particular, this means that the left end of the left beam is clamped. Then, the following fully discrete numerical formulation holds in the distributional sense; for $i = 1, 2$,

$$
\begin{aligned}
\frac{1}{h_t}&(v_{ih_t,h_x}^{k+1} - v_{ih_t,h_x}^k) \\
&= -\frac{k_i}{2}(\omega_{ih_t,h_x}^{k+1} + \omega_{ih_t,h_x}^k) + (-1)^{i+1}\sigma_{ih_t,h_x}^k \\
&\quad - \frac{d_i}{2}\Big((\omega_{ih_t,h_x}^k)_t + (\omega_{ih_t,h_x}^{k+1})_t\Big) + \Big(((u_{ih_t,h_x}^k)')^2 - \bar{\nu}\,p^k\Big)(u_{ih_t,h_x}^k)'',
\end{aligned}
\tag{7.3}
$$

$$\omega_{ih_t,h_x}^k = (u_{ih_t,h_x}^k)'''', \quad (\omega_{ih_t,h_x}^k)_t = (v_{ih_t,h_x}^k)'''', \tag{7.4}$$

$$\frac{1}{h_t}(u_{ih_t,h_x}^{k+1} - u_{ih_t,h_x}^k) = \frac{1}{2}(v_{ih_t,h_x}^{k+1} + v_{ih_t,h_x}^k). \tag{7.5}$$

By the contact condition (2.8) the numerical approximation of contact forces becomes $\sigma_{h_t,h_x}^k = \sigma_{1h_t,h_x}^k = -\sigma_{2h_t,h_x}^k$.

We turn to the contact of the two Gao beams at the joint. The contact at $x = x_{i_*}$ is described by the normal compliance condition (2.14), where we set $\lambda = \lambda_1 = \lambda_2$, thus at $t = t_k$,

$$
\begin{aligned}
\sigma_{h_t,h_x}^k := \sigma_{h_t,h_x}(t_k) &= \lambda(u_{2h_t,h_x}^{k+1}(x_{i_*}) - u_{1h_t,h_x}^{k+1}(x_{i_*}) - g_2)_+ \\
&\quad - \lambda(u_{1h_t,h_x}^{k+1}(x_{i_*}) - u_{2h_t,h_x}^{k+1}(x_{i_*}) - g_1)_+,
\end{aligned}
\tag{7.6}
$$

where the normal compliance stiffness coefficient $\lambda > 0$ is likely to be large.

As can be seen, over the time interval $[0, T]$, we use a hybrid of three numerical schemes: for the elasticity and viscosity the midpoint rule is applied and for the contact conditions the implicit Euler method is used, and for the nonlinear term in the equation of motion the central difference formula is applied. The fully discrete approximation of the displacement, $\mathbf{u}_{h_t,h_x}$ is a linear interpolant with

$$\mathbf{u}_{h_t,h_x}(\cdot, t_k) = \mathbf{u}_{h_x}^k, \quad \text{and} \quad \mathbf{u}_{h_t,h_x}(\cdot, t_{k+1}) = \mathbf{u}_{h_x}^{k+1},$$

and the fully discrete approximation of the velocity $\mathbf{v}_{h_t,h_x}$ is a constant interpolant with $\mathbf{v}_{h_t,h_x}(\cdot, t) = \mathbf{v}_{h_x}^{k+1}$ for $t \in (t_k, t_{k+1}]$. We regard the nonlinear term $((\mathbf{u}_{h_t,h_x}^k)')^2$ as the square of a strong derivative, so we apply the central difference formula into it. Thus, at each time step $t_k = k\,h_t$, we deal with the following numerical differentiations, at $x = x_i$,

$$\Big((u_{1h_t,h_x}^k)'\Big)^2 = \Big(\frac{u_{1i+1}^k - u_{1i-1}^k}{2h_x}\Big)^2, \quad \Big((u_{2h_t,h_x}^k)'\Big)^2 = \Big(\frac{u_{2i+1}^k - u_{2i-1}^k}{2h_x}\Big)^2.$$

Next, we set up the linear system associated with the nonlinear term. The coefficient matrix, at each time step $t = t_k$, has the form

$$\mathbf{L}_1^k \equiv (L_1^k)_{ij} = \int_0^{l_*} \psi_{1,i}'(x)\psi_{1,j}'(x)\Big(a_1\Big(\frac{u_{1i+1}^k - u_{1i-1}^k}{2h_x}\Big)^2 - \bar{\nu}\,p^k\Big)dx,$$

$$\mathbf{L}_2^k \equiv (L_2^k)_{ij} = \int_{l_*}^l \psi_{1,i}'(x)\psi_{1,j}'(x)\Big(a_2\Big(\frac{(u_{2i+1}^k - u_{2i-1}^k)}{2h_x}\Big)^2 - \overline{\nu}\,p^k\Big)dx.$$

Thus, we obtain the tridiagonal finite element coefficient matrix. The main diagonal is assembled in the way that if $i = j$, $(L_1^k)_{ij} = \varsigma_{i-1}^k + \varsigma_i^k$ for $1 \le i \le i_*$. The two subdiagonals are assembled as follows; if $j = i+1$ or $(L_1^k)_{ij} = -\varsigma_i^k$ for $1 \le i \le i_* - 1$ and if $i = j+1$ or $(L_1^k)_{ij} = -\varsigma_i^k$ for $1 \le j \le i_* - 1$. If $|i - j| > 1$, $(L_1^k)_{ij} = 0$. Here each element of the symmetric matrix L_{ij}^k with $1 \le i, j \le i_*$ is defined by

$$\varsigma_i^k = \int_{x_i}^{x_{i+1}} \Big(a_1\Big(\Big(fracu_{1i+1}^k - u_{1i-1}^k 2h_x\Big)^2 - \overline{\nu}\,p^k\Big)dx$$
$$= \frac{a_1(u_{1i+1}^k - u_{1i-1}^k)^2}{4h_x} - \overline{\nu}\,p^k h_x.$$

Similarly, the coefficient matrix $\mathbf{L}_2^k$ can be assembled at each time step $t = t_k$. When we compute the next step solutions $(\mathbf{u}_{h_x}^{k+1}, \mathbf{v}_{h_x}^{k+1})$ satisfying the fully discrete formulations (7.3)–(7.5), we multiply both sides of (7.3) by the basis functions $\psi_{1,i}(x)$ and apply integration by parts, thus,

$$\begin{pmatrix} \frac{1}{h_t}\sum_{j=1}^{i_*}(v_{1j}^{k+1} - v_{1j}^k)\int_0^{l_*}\psi_{1,j}(x)\psi_{1,i}(x)dx \\ \frac{1}{h_t}\sum_{j=i_*}^{m-1}(v_{2j}^{k+1} - v_{2j}^k)\int_{l_*}^0\psi_{1,j}(x)\psi_{1,i}(x)dx \end{pmatrix} = \begin{pmatrix} \mathbf{D}_1 \\ \mathbf{D}_2 \end{pmatrix}, \tag{7.7}$$

where

$$\mathbf{D}_1 = -\frac{k_1}{2}\sum_{j=1}^{i_*}(\omega_{1j}^{k+1} + \omega_{1j}^k)\int_0^l \psi_{0,j}(x)\psi_{1,i}(x)dx$$
$$- \frac{d_1}{2}\sum_{j=1}^{i_*}(\varpi_{1i}^k + \varpi_{1i}^k)\int_0^l \psi_{0,j}(x)\psi_{1,i}(x)dx + \boldsymbol{\sigma}_1^k \tag{7.8}$$
$$- \sum_{j=1}^{i_*}\Big(a_1\Big(\frac{u_{1j+1}^k - u_{1j-1}^k}{2h_x}\Big)^2 - \overline{\nu}\,p^k\Big)u_{1j}^k\int_0^l \psi_{1,j}'(x)\psi_{1,i}'(x)dx,$$

and

$$\mathbf{D}_2 = -\frac{k_2}{2}\sum_{j=i_*}^{m-1}(\omega_{2j}^{k+1} + \omega_{2j}^k)\int_0^l \psi_{0,j}(x)\psi_{1,i}(x)dx$$
$$- \frac{d_2}{2}\sum_{j=i_*}^{m-1}(\varpi_{2i}^k + \varpi_{2i}^k)\int_0^l \psi_{0,j}(x)\psi_{1,i}(x)dx - \boldsymbol{\sigma}_2^k \tag{7.9}$$
$$- \sum_{j=i_*}^{m-1}\Big(a_2\Big(\frac{u_{2j+1}^k - u_{2j-1}^k}{2h_x}\Big)^2 - \overline{\nu}\,p^k\Big)u_{2j}^k\int_0^l \psi_{1,j}'(x)\psi_{1,i}'(x)dx.$$

The substitutions $\omega_{h_t,h_x}^k = (\mathbf{u}_{h_t,h_x}^k)''''$, and $(\varpi_{h_t,h_x}^k)_t = (\mathbf{v}_{h_t,h_x}^k)''''$ in the equation (7.4) allow us to obtain the following intermediate equations:

$$\sum_{j=1}^{i_*}\omega_{1j}^k\int_0^l \psi_{0,j}(x)\psi_{3,i}(x)dx = \sum_{j=1}^{i_*}u_{1j}^k\int_0^l \psi_{3,j}''(x)\psi_{3,i}''(x)dx, \tag{7.10}$$

and

$$\sum_{j=1}^{i_*} \omega_{2j}^k \int_0^l \psi_{0,j}(x)\psi_{3,i}(x)dx = \sum_{j=1}^{i_*} u_{2j}^k \int_0^l \psi_{3,j}''(x)\psi_{3,i}''(x)dx. \qquad (7.11)$$

Since the volumes of the linear and the cubic B-splines near each node are equal, it follows that, for $1 \le j \le m-1$,

$$\int_0^l \psi_{1,j}(x)\,dx = \int_0^l \psi_{3,j}(x)\,dx. \qquad (7.12)$$

Thus, it follows from (7.7)–(7.12) that the linear system corresponding to equation (7.7) can be written as follows,

$$\begin{pmatrix} \frac{1}{h_t}\mathbf{M}_1(\mathbf{v}_1^{k+1} - \mathbf{v}_1^k) \\ \frac{1}{h_t}\mathbf{M}_2(\mathbf{v}_2^{k+1} - \mathbf{v}_2^k) \end{pmatrix} = \begin{pmatrix} \mathbf{D}_1 \\ \mathbf{D}_2 \end{pmatrix},$$

where

$$\mathbf{D}_1 = -\frac{k_1}{2}\mathbf{K}_1(\mathbf{u}_1^{k+1} + \mathbf{u}_1^k) - \frac{d_1}{2}\mathbf{K}_1(\mathbf{v}_1^{k+1} + \mathbf{v}_1^k) - \mathbf{L}_1^k\mathbf{u}_1^k + \boldsymbol{\sigma}_1^k,$$

$$\mathbf{D}_2 = -\frac{k_2}{2}\mathbf{K}_2(\mathbf{u}_2^{k+1} + \mathbf{u}_2^k) - \frac{d_2}{2}\mathbf{K}_2(\mathbf{v}_2^{k+1} + \mathbf{v}_2^k) - \mathbf{L}_1\mathbf{u}_2^k - \boldsymbol{\sigma}_2^k.$$

Here,

$$\mathbf{u}_1^k = (u_{11}^k, u_{12}^k, \ldots, u_{1i-1}^k, u_{1i_*}^k)^T, \quad \mathbf{u}_2^k = (u_{2i_*}^k, u_{2i_*+1}^k, \ldots, u_{2m-2}^k, u_{2m-1}^k)^T,$$

$$\mathbf{v}_1^k = (v_{11}^k, v_{12}^k, \ldots, v_{1i_*-1}^k, v_{1i_*}^k)^T, \quad \mathbf{v}_2^k = (v_{2i_*}^k, v_{2i_*+1}^k, \ldots, v_{2m-2}^k, v_{2m-1}^k)^T,$$

$$\boldsymbol{\sigma}_1^k = (0,0,\ldots,0,\sigma_{h_t,h_x}^k)^T, \quad \boldsymbol{\sigma}_2^k = (\sigma_{h_t,h_x}^k, 0, \ldots, 0)^T.$$

The symmetric matrices $\mathbf{M}_1$, $\mathbf{M}_2$, $\mathbf{K}_1$, and $\mathbf{K}_2$ are defined by

$$\mathbf{M}_1 \equiv (M_1)_{ij} = \int_0^{l_*} \psi_{1,i}(x)\psi_{1,j}(x),$$

$$\mathbf{M}_2 \equiv (M_2)_{ij} = \int_{l_*}^l \psi_{1,i}(x)\psi_{1,j}(x)\,dx,$$

$$\mathbf{K}_1 \equiv (K_1)_{ij} = \int_0^{l_*} \psi_{3,i}''(x)\psi_{3,j}''(x)\,dx,$$

$$\mathbf{K}_2 \equiv (K_2)_{ij} = \int_{l_*}^l \psi_{3,i}''(x)\psi_{3,j}''(x)\,dx,$$

and they are banded with three subdiagonals and superdiagonals. From the extra equation (7.5), we find

$$\frac{1}{h_t}\sum_{j=1}^{i_*}(u_{1j}^{k+1} - u_{1j}^k)\int_0^l \psi_{1,j}(x)\psi_{1,i}(x)dx = \frac{1}{2}\sum_{j=1}^{i_*}(v_{1j}^{k+1} + v_{1j}^k)\int_0^l \psi_{1,j}(x)\psi_{1,i}(x)dx,$$

and

$$\frac{1}{h_t}\sum_{j=i_*}^{m-1}(u_{2j}^{k+1} - u_{2j}^k)\int_0^l \psi_{1,j}(x)\psi_{1,i}(x)dx = \frac{1}{2}\sum_{j=i_*}^{m-1}(v_{2j}^{k+1} + v_{2j}^k)\int_0^l \psi_{1,j}(x)\psi_{1,i}(x)dx.$$

Now, we can use (7.5) to set up the linear system that marches the solution one time step, for $\iota = 1, 2$

$$
\begin{aligned}
\mathbf{u}_\iota^{k+1} = {}& \Big(\frac{2}{h_t^2} \mathbf{M}_\iota + (\frac{k_\iota}{2} + \frac{d_i}{h_t}) \mathbf{K}_\iota \Big)^{-1} \\
& \times \Big(\Big(\frac{2}{h_t^2} \mathbf{M}_\iota - (\frac{k_\iota}{2} - \frac{d_i}{h_t}) \mathbf{K}_\iota - \mathbf{L}_\iota^k \Big) \mathbf{u}_\iota^k + \frac{2}{h_t} \mathbf{M}_\iota \mathbf{v}_\iota^k + (-1)^{\iota+1} \boldsymbol{\sigma}_\iota^k \Big).
\end{aligned}
\tag{7.13}
$$

We note that this linear system does not yet satisfy the normal compliance contact condition (7.6). So, we introduce additional notation to deal with the condition and that will allow us to compute the next step solutions $\mathbf{u}_\iota^{k+1}$ which satisfy (7.6) and (7.13).

Consider a matrix $\mathbf{A} \in \mathbb{R}^{i_* \times (m-1-i_*)}$. Then the notation of block matrices is as follows. If $1 \le i_1 \le i_2 \le i_*$ and $1 \le j_1 \le j_2 \le m-1-i_*$, i.e., we extract i_1th row to i_2th row and j_1th column to j_2th column, the block matrix is denoted by $A(i_1 : i_2, j_1 : j_2) \in \mathbb{R}^{(i_2-i_1-1) \times (j_2-j_1-1)}$. We use the following substitutions in the linear system (7.13) to simply the matrices involved,

$$
\mathbf{B}_\iota = \frac{2}{h_t^2} \mathbf{M}_\iota + (\frac{k\iota}{2} + \frac{d_\iota}{h_t}) \mathbf{K}_\iota,
$$

$$
\mathbf{Q}_\iota^k = \frac{2}{h_t^2} \mathbf{M}_\iota - (\frac{k_\iota}{2} - \frac{d_\iota}{h_t}) \mathbf{K}_\iota - \mathbf{L}_\iota^k.
$$

Note that the matrix $\mathbf{Q}_\iota^k$ changes at each time step $t = t_k$. Next, algebraic manipulations allow us to obtain the normal compliance in terms of only $u_{1i_*}^{k+1}$ and $u_{2i_*}^{k+1}$, indeed, we can write

$$
q_1 u_{1i_*}^{k+1} - b_1^k = \lambda(u_{1i_*}^{k+1} - u_{2i_*}^{k+1} - g_1)_+, \tag{7.14}
$$

$$
q_2 u_{2i_*}^{k+1} - b_2^k = \lambda(u_{2i_*}^{k+1} - u_{1i_*}^{k+1} - g_2)_+, \tag{7.15}
$$

where

$$
\begin{aligned}
q_1 = {}& (B_1)_{i_* i_*} - B_1(i_*, 1 : i_* - 1)[B_1(1 : i_* - 1, 1 : i_* - 1)]^{-1} \\
& \times B_1(1 : i_* - 1, i_*), \\
b_1^k = {}& -B_1(i_*, 1 : i_* - 1) \times [B_1(1 : i_* - 1, 1 : i_* - 1)]^{-1} \\
& \times (Q_1^k(1 : i_* - 1, 1 : i_*) \mathbf{u}_1^k + \frac{2}{h_t} M_1(1 : i_* - 1, 1 : i_*) \mathbf{v}_1^k) \\
& + Q_1^k(i_*, 1 : i_*) \mathbf{u}_1^k + \frac{2}{h_t} M_1(i_*, 1 : i_*) \mathbf{v}_1^k, \\
q_2 = {}& (B_2)_{i_* i_*} - B_2(i_*, i_* + 1 : m - 1) \\
& \times [B_1(i_* + 1 : m - 1, i_* + 1 : m - 1)]^{-1} B_1(i_* + 1 : m - 1, i_*), \\
b_2^k = {}& -B_2(i_*, i_* : m - 1) \times [B_1(i_* : m - 1, i_* : m - 1)]^{-1} \\
& \times \Big(Q_2^k(i_* : m - 1, i_* : m - 1) \mathbf{u}_2^k + \frac{2}{h_t} M_2(i_* : m - 1, i_* : m - 1) \mathbf{v}_1^k \Big) \\
& + Q_2^k(i_*, i_* : m - 1) \mathbf{u}_2^k + \frac{2}{h_t} M_2(i_*, i_* : m - 1) \mathbf{v}_2^k.
\end{aligned}
$$

Once $u_{1i_*}^{k+1}$ and $u_{2i_*}^{k+1}$ have been computed from (7.14) and (7.15), the next step solutions $\mathbf{u}_1^{k+1}$ and $\mathbf{u}_2^{k+1}$ can be computed. Excluding the last component of $\mathbf{u}_1^{k+1}$

and the first component of $\mathbf{u}_2^{k+1}$, we let

$$\mathbf{x}_1^{k+1} = (u_{11}^{k+1}, u_{12}^{k+1}, \ldots, u_{1i_*-2}^{k+1}, u_{1i_*-1}^{k+1}) \in \mathbb{R}^{i_*-1},$$
$$\mathbf{x}_2^{k+1} = (u_{2i_*+1}^{k+1}, \ldots, u_{2i_*+2}^{k+1}, \ldots, u_{2m-1}^{k+1}, u_{2m-2}^{k+1}) \in \mathbb{R}^{m-i_*}.$$

Then

$$\begin{aligned}
\mathbf{x}_1^{k+1} = [B_1(1; i_* - 1, 1; i_* - 1)]^{-1} \Big(& Q_1^k(1; i_* - 1, 1; i_*) \mathbf{u}_1^k \\
& + \frac{2}{h_t} M_1(1; i_* - 1, 1; i_*) \mathbf{v}_1^k - Q_1^k(1; i_* - 1, i_*) u_{1i_*}^{k+1} \Big),
\end{aligned} \tag{7.16}$$

$$\begin{aligned}
\mathbf{x}_2^{k+1} = [B_1(i_*; m, i_*; m)]^{-1} \Big(& Q_2^k(i_* + 1; m, i_*; m) \mathbf{u}_2^k \\
& + \frac{2}{h_t} M_2(i_* + 1; m, i_*; m) \mathbf{v}_2^k - Q_2^k(i_* + 1; m, i_*) u_{2i_*}^{k+1} \Big).
\end{aligned} \tag{7.17}$$

At the final step, the actual approximation of u_1 is computed.

The discussion above can be summarized as the following algorithm.

Algorithm 7.1. Assume that initial data $\mathbf{u}_1^0$ and $\mathbf{u}_2^0$ are given and $\lambda > 0$ is sufficiently large.
for $k = 1 : T/h_t$
     the previous solution $(\mathbf{u}_1^{k-1}, \mathbf{u}_2^{k-1})^T$ is known
     Compute $(\mathbf{u}_1^k, \mathbf{u}_2^k)^T$ using the linear system (7.13)
     Compute $(u_{1i_*}^{k+1}, u_{2i_*}^{k+1})$ using (7.14) and (7.15)
if $u_{1i_*}^k - u_{2i_*+1}^k < g_1$ **and** $u_{2i_*+1}^k - u_{1i_*}^k < g_2$
     $\sigma^{k-1} \leftarrow 0$, $u_{1i_*}^k \leftarrow b_1/q_1^{k-1}$, $u_{2i_*+1}^k \leftarrow b_2/q_2^{k-1}$ from (7.14)–(7.15)
else if $g_1 \leq u_{1i_*}^k - u_{2i_*+1}^k \leq g_1 + 1/\lambda$
     compute $(u_{1i_*}^k, u_{2i_*}^k)$ from (7.14) and (7.15) and then

$$\sigma^k \leftarrow -\lambda(u_{1i_*}^{k+1} - u_{2i_*}^{k+1} - g_1)_+$$

else if $g_2 \leq u_{2i_*+1}^k - u_{1i_*}^k \leq g_2 + 1/\lambda$ compute $(u_{1i_*}^k, u_{2i_*}^k)$ from (7.14) and (7.15) and then

$$\sigma^k \leftarrow \lambda(u_{2i_*}^{k+1} - u_{1i_*}^{k+1} - g_2)_+$$

end if
     Compute $(\mathbf{u}_1^k, \mathbf{u}_2^k)$ by using (7.16) and (7.17).
     Compute $(\mathbf{v}_1^k, \mathbf{v}_2^k)$ from the following identities

$$\mathbf{v}_1^k = \frac{2}{h_t}(\mathbf{u}_1^k - \mathbf{u}_1^{k-1}) - \mathbf{v}_1^{k-1}, \quad \mathbf{v}_2^k = \frac{2}{h_t}(\mathbf{u}_2^k - \mathbf{u}_2^{k-1}) - \mathbf{v}_2^{k-1}$$

end for

The algorithm was implemented and a typical run took on the average 0.1274 seconds to compute one time step for the solutions with $p = 0$ and an average of 0.1259 seconds to compute each time step in the case of $p = 895$. The numerical analysis of the algorithm is currently under study in [4].

8. Numerical Results

In this section we present results of preliminary numerical simulations obtained by using a code based on the algorithm described in the previous section. We show two sets of simulations that depict some of the behaviors of the system. Following the simulations, we make a few remarks on the possible types of behavior and

on the implementation. Our main interest is in the simulations of the dynamic behavior of the system in two cases: $p = 0$, in which there is no buckling, and $p = 895$, in which there is buckling. This is a preliminary study of the transmission of vibrations across joints between two Gao beams. As can be seen below, even the two 'simple' cases are not simple and lead to very complicated behavior. Therefore, a further in-depth study of the numerics has merit in and of itself.

The two simulations are of two long beams made of steel. For the sake of simplicity, we assumed that the viscosity is negligible and set $d_1 = d_2 = 0$. We assumed that no forces acted on the beams; i.e., $f_1 = f_2 = 0$, and let $\Phi = 0$. Indeed, when the left end of the left beam is clamped to a stationary device, $\phi = 0$ and the shift with Φ is not needed. Therefore, the equations of the two Gao beams are,

$$u_{1tt} + k_1 u_{1xxxx} + (\overline{\nu}_1 p - a_1 u_{1x}^2) u_{1xx} = 0,$$
$$u_{2tt} + k_2 u_{2xxxx} + (\overline{\nu}_2 p - a_2 u_{2x}^2) u_{2xx} = 0.$$

Table 1: Input data (dimensionless)

L_1	L_2	k_1	k_2	$\overline{\nu}_1 = \overline{\nu}_2$	λ	a_1	a_2	$g_1 = g_2$
0.5	0.5	14.7	7.35	1.30	10^4	40	110	4×10^{-7}

The input data (in dimensionless form) is provided in Table 1. We note that the stops are relatively very rigid, the left beam is twice as stiff as the right one, the Gao coefficients are large, and the gap is very small.

In the first simulation the horizontal traction is $p = 0$, and so we do not expect bucking of the two beams. In the second simulation the horizontal traction is $p = 895$ which allows for buckling. Moreover, we assumed that $l_* = 0.5$, so the two beams are of equal length. The fact that the left beam is stiffer than the right one causes asymmetrical behavior that is clearly seen in the simulations. We used the normal compliance contact condition with very large stiffness ($\lambda = 10^4$). The case of the Signorini contact condition was deemed not realistic and was not simulated.

The initial displacements and velocities of the beams were, respectively,

$$u_{01}(x) = 2.5 \cdot 10^{-5} x^3, \quad v_{01}(x) = 0, \quad 0 \leq x \leq 0.5,$$
$$u_{02}(x) = -2.5 \cdot 10^{-5}(x-1)^3, \quad v_{02}(x) = 0, \quad 0.5 \leq x \leq 1.$$

Both displacements were very small and there was no contact initially, also, the the vibrations started from rest.

We now describe the numerical experiments. The size of the subinterval, i.e., the space step, was $h_x = 2 \times 10^{-4}$ and the time step was $h_t = 1 \times 10^{-4}$. We computed the solution over 1×10^4 time steps, that is over the time interval $0 \leq t \leq 1$. At each time step the 2500×2500 linear system, composed of band matrices, was computed by using the sparse matrix function in MATLAB, which is based on the Gaussian elimination. This allowed us to save memory by compressing the zero elements in the band matrices.

In the actual computations, about 1275 seconds of real time elapsed for the results in the case $p = 0$ and over 1260 seconds in the case of $p = 895$. Therefore,

the average time to compute one step of the numerical solutions was approximately 0.126 second.

The system started without contact, and in the case $p = 0$ the first contact was at the upper stop at about $t = 0.4546$, and for $p = 895$ the first contact was also at the upper stop at about $t = 0.4490$. Then, the oscillations exhibited a slower wave that moved from the joint to the ends, upon which oscillations with higher frequency were superimposed.

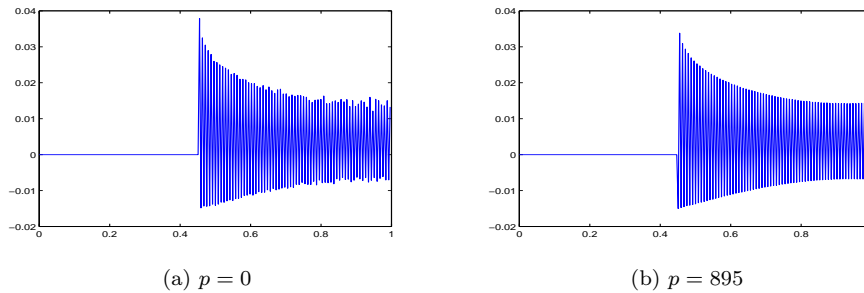(a) $p = 0$ (b) $p = 895$

Figure 8.1: Contact forces for $0 \leq t \leq 1$

The contact force, computed from the normal compliance condition (7.14) and (7.15), is displayed in Figure 8.1. The sampling was done at every 41 time steps. It reflects a very interesting feature of both simulations, namely, up to about $t = 0.45$ the amplitude of the oscillations was comparable to the initial displacements, and then, once first contact was established, the amplitude switched to about .04 and then decreased to about 0.02, where it stabilized. We see that once contact started, the left beam's end oscillated and contacted both stops consecutively, and that the contact stress was negative at the top stop and positive at the bottom stop. The contact stress amplitude in both cases shows a very similar trend and magnitude. However, the oscillations in the case $p = 895$ were more orderly.

The displacements behaved in a way that is very different from that of the related linear beams ($a_1 = a_2 = 0$). Indeed, in addition to the buckling of the right beam, the oscillations were quite complex, as can be seen in Figure 8.2.

The displacements of the two beams at six different times in the interval $0 < t \leq 0.45$ are depicted in parts (a) and (b) of Figure 8.2. The left beam (which is stiffer) oscillates about $u_1 = 0$, that is its zero equilibrium state, while the right beam (which is softer) oscillates about a buckled state. In both cases small amplitude high frequency oscillations are superimposed on the main ones. We note that the scale is 10^{-6}, which is the same as the scale of the initial displacements. Next, i(c) and (d) show the displacements of the two beams at six different times in the time interval $0.45 < t \leq 0.75$. Here, the scale is 10^{-3} for the left beam and 10^{-5} for the right one. The left beam is oscillating about the zero equilibrium state with a much higher amplitude, while the right beam is oscillating about a buckled state. Again, small amplitude high frequency oscillations are superimposed on the main ones. Finally, (e) and (f) depict the displacements of the two beams at 6 different times in the interval $0.75 < t \leq 1$. The scale is 10^{-3} for the left beam that oscillates

(a) $0 < t \leq 0.45$

(b) $0 < t \leq 0.45$

(c) $0.45 < t \leq 0.75$

(d) $0.45 < t \leq 0.75$

(e) $0.75 < t \leq 1$
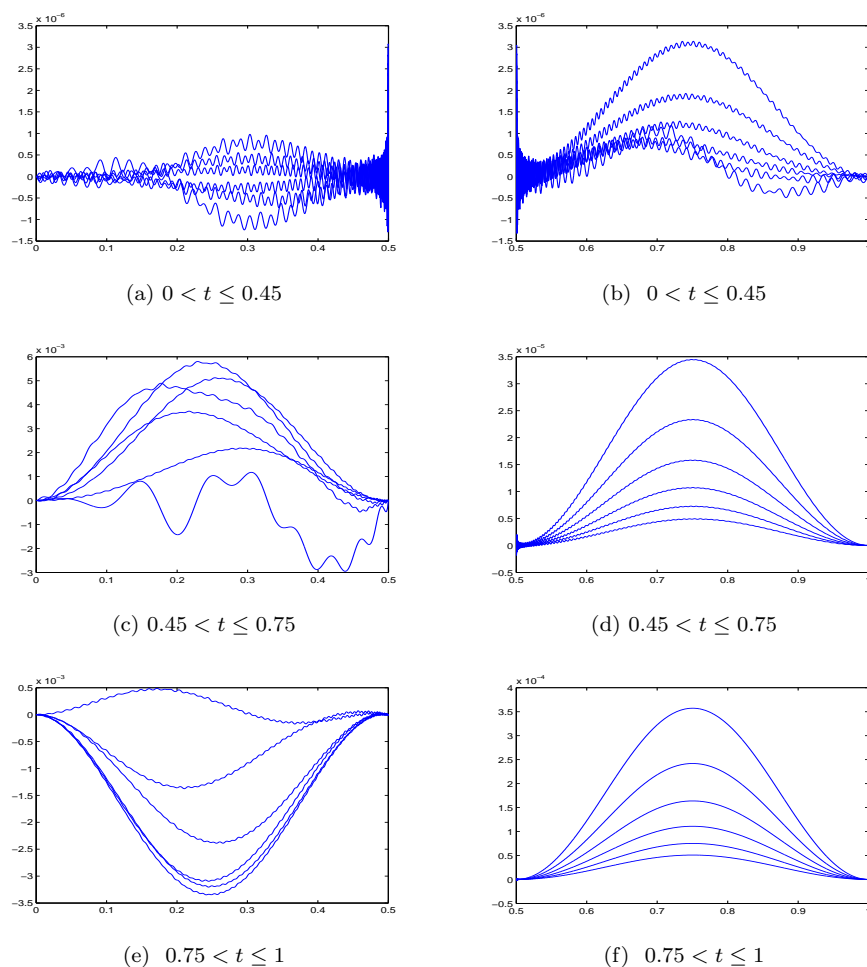
(f) $0.75 < t \leq 1$

Figure 8.2: Displacements of the beams (left and right) about three different times, $p = 895$

about the zero state., while the scale is 10^{-4} for the right beam, and it oscillates about its buckled state. However, there are no small amplitude high frequency oscillations that were observed earlier.

As was noted above, the difference in the beams' behavior is related to the difference in their stiffness and the Gao coefficient (a_1 and a_2 in Table 1). Concerning the small amplitude high frequency oscillations, at this stage it is not clear if these are just 'noise,' since they seem to be very regular, therefore, additional investigation is needed to determine if these are 'real' or just numerical noise.

We now describe the frequency spectrum or the 'noise' characteristics of the system. To that end we present the Fast Fourier Transform (FFT) of the displacements $u_1(0.25, t)$ and $u_2(0.75, t)$ in Figs. 8.3 and 8.4. These provide the system behavior in the frequency domain.

(a) left beam

(b) right beam
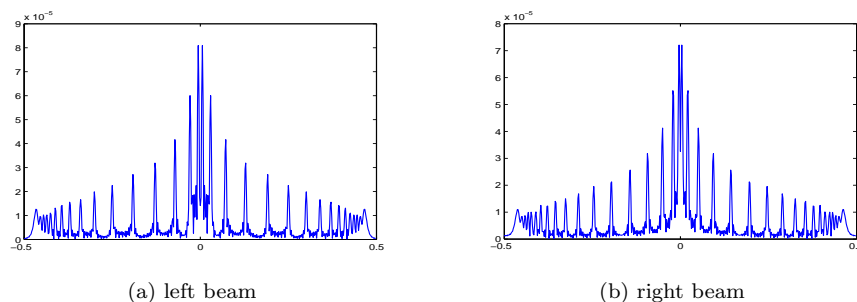
Figure 8.3: The frequency spectrum (FFT) of the beams, $p = 0$

(a) left beam

(b) right beam
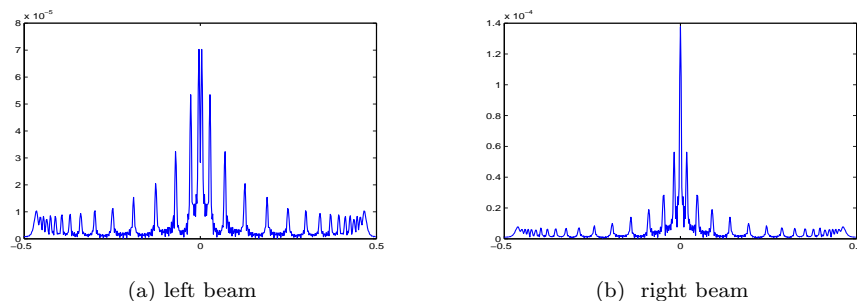
Figure 8.4: The frequency spectrum (FFT) of the beams, $p = 895$

The number of points in the FFT is $f_s = 512$, and the scale has been normalized so the frequency is in between 0 and 1, also the sample was of 200 signals. We depict the frequencies in $[-0.5, 0.5]$ to better capture the signal near the origin.

It is seen in the case $p = 0$, Figure 8.3, that the main two frequencies lie near zero, but there are many activated frequencies, and also the spectrum near 0.5 is quite dense. It is noted that the system is rather noisy, with many small amplitude frequencies present.

Next, Figure 8.4 depicts the FFT of the motion of the two beams in the case of $p = 895$. The FFT is similar the one in the first case, but the central peak and the second peak are much more pronounced in the right beam, indeed, they are an order of magnitude larger. On the other hand the other frequencies are distributed somewhat differently.

We note that the presence of contact between the beams makes the results much more noisy. Indeed, as is indicated in the FFT, a whole spectrum of frequencies is present, which means plenty of noise. A further study is warranted to determine how much of the noise is numerical.

As was pointed above, these numerical experiments are preliminary and they open a whole new direction for research, and more will be done in our future

studies. An interesting set would be the study of the motion when one beam is vibrating about an upper buckled state and the other one about a lower state.

9. Conclusions

This work studies the vibrations of two nonlinear Gao beams that are connected via a joint in which there are two stops at the left end of the right beam with a clearance between them (see Figs. 2.1 and 2.2). The right end of the left beam is constrained to move within this clearance. The motivation for the study is our long-term goal of studying the transmission of vibrations across joints. The interest in using the Gao beam model arises from the fact that it can naturally predict oscillations about a buckled steady state.

The process was modeled using the system (2.1)–(2.10) when contact was modeled with the *normal compliance contact condition,* which means that the stops were reactive. When the stops were perfectly rigid, contact was modeled with the *Signorini nonpenetration condition,* and the system consisted of (2.1)–(2.8), (2.10) and (2.13)–(2.14).

The existence of the unique weak solution of the problem with the normal compliance condition was stated in Theorem 3.1 and established in Section 4. The main issue was to deal with the cubic term $(u_x)^3$ in the variational formulation. The existence of the weak solution to the problem with the Signorini condition was stated in Theorem 3.2, and shown in Section 5. It was based on obtaining a priori estimates on the solutions of the problem with the normal compliance condition and passing to the limit when the normal compliance stiffness tends to infinity. As usual, the question of the uniqueness of the solutions remains unresolved. The existence of weak solutions to the respective problems without viscosity were obtained in Section 6, again, as the limits of convergent sequences of solutions with viscosity when the viscosity coefficients vanish.

The mathematical and numerical difficulties associated with the Signorini contact condition are very challenging, and it seems to us of very little applied relevance, since there are no perfectly rigid materials or stops. In passing we just mention that, in addition to the weak regularity of the solutions with this condition, the non-uniqueness seems to be related to the fact that following contact there is no clear rule about the rebound, which often is masked by supplementing the so-called *restitution coefficient.*

The numerical algorithm for the computer simulations of the model with the normal compliance condition was developed in Section 7. It is a fully discrete numerical method and uses a uniform discretization of the time interval $[0, T]$ and a mixture of the Galerkin approximation and central difference formula to discretize the space interval $[0, 1]$. The central difference formula is combined with the finite element method (FEM) when we deal with the nonlinear Gao terms in the two equations. The basis functions for the FEM were piecewise linear and piecewise cubic splines, with special attention to the two elements on both sides of the joint. The normal compliance contact condition was implemented by using an implicit discretization. The weak formulation led to a linear system that was sparse and solved using (7.13). The convergence of the algorithm is under study in [4].

Finally, the results of the numerical simulations obtained by implementing the algorithm, were presented in Section 8. We used two sets of simulations for beams with different Gao coefficients and stiffnesses. In the first set the applied horizontal

traction was $p = 0$, so the beams oscillated about the zero equilibrium. The oscillations were quite interesting and there was superposition of fast frequencies on top of the basic frequency. The vibrational spectrum, or the noise characteristics in this case, depicted in Figure 8.3, is seen to be quite noisy. In the second case of $p = 895$, the right beam was in a buckled state and the left beam was not. As was found in [7, 26] in the case of one Gao beam, the oscillations were about the buckled state, as can be seen clearly in Figure 8.2 (b, d, f). The system was also noisy, but the basic frequency was more pronounced.

These results open the way to a thorough investigation of the vibrations transmission across joints, which, as stated in the introduction, is the long-term goal of this work. However, on the way we still need to make the implementation faster, and to run numerical experiments to get a more comprehensive understanding of the vibrations of Gao beams. Then, we plan to use the driving function $\phi = \phi(t)$ for the investigation.

Another issue of interest is to add friction to the contact condition in the joint. That is likely to make the model substantially more complex both mathematically and computationally.

References

[1] R. Adams; *Sobolev Spaces*, Academic Press, 1975.

[2] J. Ahn; *Thick obstacle problems with dynamic adhesive contact*, Math. Model. Numer. Anal. (M2AN) **42**(6) (2008), 1021–1045.

[3] J. Ahn; *A viscoelastic Timoshenko beam with Coulomb law of friction*, Appl. Math. & Computation **218** (2012), 7078–7099.

[4] J. Ahn and Eun-jae Park; *Dynamic frictionless contact of a Gao beam with two stops*, preprint.

[5] J. Ahn, and D. E. Stewart; *Euler–Bernoulli beam with dynamic contact: Discretization, convergence, and numerical results*, SIAM J. Numer. Anal. **43**(4) (2005), 1455–1480 (electronic).

[6] L.-E. Andersson; *A quasistatic frictional problem with a normal compliance penalization term*, Nonlinear Analysis **37** (1999), 689–705.

[7] K. T. Andrews, M. F. M'Bemgue, Y. Dumont, J. Purcell, and M. Shillor; *Analysis and Simulations of a Nonlinear Dynamic Beam*, ZAMP, to appear.

[8] K. T. Andrews, M. F. M'Bengue, and M. Shillor; *Vibrations of a nonlinear dynamic beam between two stops*, Discrete and Continuous Dynamical System (DCDS-B) **12**(1) (2009), 23–38.

[9] K. T. Andrews and M. Shillor; *Thermomechanical behaviour of a damageable beam in contact with two stops*, Applicable Analysis **85**(6-7) (2006), 845–865.

[10] K. T. Andrews, M. Shillor, and S. Wright; *On the dynamic Vibrations of an elastic beam in frictional contact with a rigid obstacle*, J. Elasticity, **42**(1996), 1–30.

[11] I. Babśka, J. Osborn, and J. Pitkäranta; *Anaylsis of mixed methods using mesh dependent norm*, Math. Computation **35**(152)(1980), 1039–1062

[12] D. Braess; *Finite Elements*, Cambridge University Press, 2001.

[13] S. C. Brenner and L. R. Scott; *The Mathematical Theory of Finite Element Methods*, Texts in Applied Mathematics **15**, Springer, 1994.

[14] P. G. Ciarlet; *The Finite Element Method for Elliptic Problems*, Applied Mathematics **40**, SIAM, 2002.

[15] Y. Dumont; *Some remarks on a vibro-impact scheme*, Numerical Algorithms **33**(2003), 227–240.

[16] C. Eck, J. Jarušek, and M. Krbec; *Unilateral Contact Problems,* Pure and Applied Mathematics **270**, Chapman & Hall/CRC Press, 2005.

[17] D. Y. Gao; *Nonlinear elastic beam theory with application in contact problems and variational approaches*, Mechanics Research Communications **23**(1) (1996), 11–17.

[18] D.Y. Gao; *Finite deformation beam models and triality theory in dynamical post-buckling analysis*, Intl. J. Non-Linear Mechanics **35** (2000), 103–131.

[19] D. Y. Gao; *Duality in distributed-parameter control of nonconvex and nonconservative dynamical systems with applications*, Nonlinear Dynamics and Systems Theory **6**(3)(2006), 257–279.

[20] D. Y. Gao and D. L. Russell; *An extended beam theory for smart materials applications: II Static formation problems*, Appl. Math. Optim. **38**(1)(1998), 69–94.

[21] N. Kikuchi and J. T. Oden; *Contact Problems in Elasticity*, SIAM, 1988.

[22] A. Klarbring, A. Mikelic, and M. Shillor; *On friction problems with normal compliance*, Nonlinear Analysis **13**(8) (1989), 935–955.

[23] A. Klarbring, A. Mikelic, and M. Shillor; *Frictional contact problems with normal compliance*, Intl. J. Engng. Sci. **26**(8) (1988), 811–832.

[24] K. L. Kuttler; *Dynamic friction contact problems for general normal and friction laws*, Nonlinear Analysis TMA **28**(3)(1997), 559– 575.

[25] K. L. Kuttler, A. Park, M. Shillor, and W. Zhang; *Unilateral dynamic contact of two beams*, Math. Comput. Modelling **34**(2001), 365–384.

[26] K. L. Kuttler, J. Purcell, and M. Shillor; *Analysis and simulations of a contact problem for a nonlinear dynamic beam with a crack*, Quarterly J. Mech. Appl. Math. (2011); doi: 10.1093/qjmam/hbr018

[27] K. L. Kuttler and M. Shillor; *Vibrations of a beam between two stops*, Dynamics of Continuous, Discrete and Impulsive Systems **8**(1)(2001), 93–110.

[28] K. L. Kuttler and M. Shillor; *Dynamic contact with normal compliance, wear, and discontinuous friction coefficient*, SIAM J. Math. Anal. **34**(1)(2002), 1–27.

[29] K. L. Kuttler and M. Shillor; *Regularity of solutions to a dynamic frictionless contact problem with normal compliance*, Nonlinear Analysis **59** (2004), 1063–1075.

[30] J. L. Lions; *Quelques Méthodes de Résolution des Problèmes aux Limites Non Linéaires*, Dunod, Paris, 1969.

[31] J. Machalova and H. Netuka; *Bending of a nonlinear beamreposing on an unilateral foundation*, Appl. Comput. Mechanics **5**(2011), 45–54.

[32] J. A. C. Martins and J. T. Oden; *A numerical analysis of a class of problems in elastodynamics with friction*, Comput. Meth. Appl.Mech. Engnr., **40**(1983), 327–360.

[33] M. F. M'Bengue; *Analysis of a Nonlinear Dynamic Beam with Material Damage or Contact*, Ph.D. Dissertation, Oakland University, March 2008.

[34] M. F. M'Bengue and M. Shillor; *Regularity result For the problem of vibrations of a nonlinear beam*, Electron. J. Diff. Eqns., Vol. 2008(2008), No. 27, 1–12.

[35] F. C. Moon and S. W. Shaw; *Chaotic vibration of a beam with nonlinear boundary conditions*, J. Nonlinear Mech. **18**(1983), 465–477.

[36] P. A. Raviart and M. F. Wheeler; *A mixed finite elementmethod for 2nd order elliptic problems*, in *Mathematical Aspects of the Finite Element Method*, Lecture Notes in Math., Springer, Berlin, 1977.

[37] L. Paoli and M. Schatzman; *Resonance in impact problems*,' Math. Comput. Modelling, **28**(4-8)(1998), 385–406.

[38] H. A .F. A. Santos and D. Y. Gao; *Canonical dual finite element method for solving post-buckling problems of a large deformation elastic beam*, Int. J. Nonlinear Mechanics **47**(2)(2012), 240–247,doi:10.1016/j.ijnonlinmec.2011.05.012

[39] M. Shillor, M. Sofonea, and J. J. Telega; *Models and Analysis of Quasistatic Contact*, Lecture Notes in Physics, **655**, Springer, Berlin, 2004.

[40] J. Simon; *Compact sets in the space $L^p(0,T;B)$*, Ann. Mat. Pura. Appl. **146**(1987), 65–96.

[41] P. Wriggers; *Computational Contact Mechanics,* Wiley, 2002.

Jeongho Ahn

Department of Mathematics and Statistics, Arkansas State University, State University, AR 72467, USA

E-mail address: jahn@astate.edu

Kenneth L. Kuttler

Department of Mathematics, Brigham Young University, Provo, UT 84602, USA

E-mail address: klkuttle@math.byu.edu

Meir Shillor
Department of Mathematics and Statistics, Oakland University, Rochester, MI 48309, USA
    E-mail address: shillor@oakland.edu